Volume 2, Issue 2, 2024

Print ISSN: 2959-9865
Online ISSN: 2959-9873

# WORLD JOURNAL OF ENGINEERING RESEARCH

# World Journal of Engineering Research

Volume 2, Issue 2, 2024


Published by Upubscience Publisher

**World Journal of Engineering Research**
**Print ISSN: 2959-9865 Online ISSN: 2959-9873**
**Email: info@upubscience.com**
**Website: http://www.upubscience.com/**

# Table of Content

**World Journal of Engineering Research**
**ISSN: 2959-9873**
**DOI: 10.61784/wjerv2n235**

# METHODS FOR DETECTING AND EARLY WARNING OF DRILLING ENGINEERING ACCIDENTS

Alexey Nikita
*Gazprom Neft Science & Technology Center, Russia.*

**Abstract:** As a very important part of engineering construction, drilling engineering has certain difficulties in terms of work content and construction technology. The quality of the project is difficult to control, and the safety factor is not high. Drilling engineering accident detection and early warning is a very critical part of engineering construction. It is an important method to ensure the quality of drilling engineering and an important measure to improve the level and safety of drilling construction. On this basis, the article will analyze drilling engineering accident detection and early warning methods to provide guarantee for the development of drilling engineering.
**Keywords:** Drilling engineering; Accident detection; Early warning method

## 1 FACTORS AND CURRENT SITUATION CAUSING DRILLING ENGINEERING ACCIDENTS

With the continuous development of social economy, the demand for petroleum resources in social production and life is increasing, the consumption of petroleum resources is also increasing year by year, and the work intensity of drilling projects is also gradually increasing. As the main method of oil extraction, drilling engineering is characterized by high risks and harsh environment. Once a drilling accident occurs, it will cause huge economic losses. Therefore, in order to ensure the quality of oil extraction, accident detection and early warning work need to be fully implemented to minimize the mining accident rate, which has positive significance for promoting the development of drilling engineering[1].

In the implementation of drilling projects, terrain and man-made factors are the main influencing factors causing drilling engineering accidents. On the one hand: terrain factors. In the development of drilling projects, terrain is a very dangerous factor. Complex and changeable terrain will affect the smooth operation of drilling work to a certain extent. In addition, if the geographical environment is harsh and the underground rocks are chaotically distributed, it will also cause damage to the drilling equipment and affect the construction quality of the drilling project. On the other hand: the human factor. Construction personnel are an important part of the drilling project and have a certain impact on the quality of the drilling project. For example, during the drilling construction process, if there are problems with the drilling staff's working ability, drilling methods, and judgment choices, it will not only affect the construction quality of the drilling project, but also cause safety accidents and hinder the normal operation of the drilling work[2]. At the same time, if the technical level of drilling construction personnel is limited and unable to cope with the complex and changeable drilling environment, it will also increase construction safety risks and hinder the improvement of drilling quality. Based on the current situation of accident detection in drilling engineering, with the continuous development of science and technology, information technology has been widely used in the development of drilling technology. Applying information technology means to drilling projects can use information technology equipment to carry out risky construction operations, reducing the probability of accidents to a certain extent[3-4]. However, in actual drilling projects, relevant detection and early warning technologies are still not perfect, and drilling engineering accidents often occur, which have an impact on the normal operation of drilling projects. For example, using engineering parameters to judge the status of the project is a commonly used detection and early warning method. However, this detection method has certain shortcomings. The flexibility and variability functions are not perfect, and it cannot effectively deal with complex drilling projects.

## 2 ANALYSIS OF DRILLING ENGINEERING ACCIDENT DETECTION AND EARLY WARNING METHODS

### 2.1 Proper Application of Drilling Instruments

Drilling instruments are common tools in drilling engineering. With the development of the oil exploration industry in recent years, drilling instruments have been improved and improved to a certain extent, and have been transformed from single detection equipment into digital equipment. At the same time, it has been integrated with microprocessing technology and remote sensing and remote control technology, and has become an important drilling tool, which is of great value to the quality of drilling engineering accident supervision[5]. Therefore, during the construction of drilling projects, drilling instruments can be reasonably installed on the drilling construction equipment to ensure that the drilling project content can be fully and effectively supervised, and real and effective drilling project data can be obtained to provide reference for fault detection and analysis[6]. Drilling technicians can conduct safety analysis based on the data provided by drilling instruments to effectively prevent accidents.

### 2.2 Application of Drilling Tool Vibration

Drilling tool vibration is an advanced drilling technology. During the construction of drilling projects, the interaction between rocks, drill bits, well walls and drill strings will cause drilling tools to vibrate. However, in the actual application process, the stress generated by the interaction between various factors is very complex[7]. It is necessary to use a MWD measuring instrument to effectively analyze the dynamic characteristics in order to fully understand the interaction forces. During the specific drilling process, the vibration conditions of the drilling tools can be analyzed to effectively monitor the working status of the drilling tools and drill bits, and prevent resonance and resonance phenomena. However, due to the limitations of the application of drilling tool vibration analysis technology, the scope and role of supervision are very small, and the application value is also relatively limited.

### 2.2 Utilizing Parameter Sensors

In drilling engineering construction, many drilling instruments are used, and parameter sensors are one of the important ones. Parameter sensors can convert the perceived drilling engineering information into specific data. For example, the felt force can be converted into pressure data; the felt water flow impact can be converted into hydraulic data. These data can help technicians judge the accuracy of the drilling project. status, showing the signal warning of the drilling project. At the same time, in drilling engineering, rational use of signal processors is also a way to improve the quality of accident early warning. When the signal processor receives the parameter sensor data, it will analyze, process and judge it, and then reflect the analysis results to the display system to provide reference for accident warning work. This can not only optimize the quality of drilling engineering data detection, but also eliminate drilling hazards in a timely manner and reduce the probability of accidents.

### 2.3 Develop Anomaly Prediction System

In the construction of drilling projects, the relevant technical departments can develop an abnormality prediction expert system, integrate fault diagnosis methods into it, and combine it with parameter sensors, signal processors and other equipment to comprehensively analyze and collect various data information to build corresponding drilling systems. The engineering anomaly prediction expert system performs early warning analysis and processing on these data. For example, the drilling engineering construction department can combine computer and artificial intelligence technologies to comprehensively utilize multiple drilling instruments and equipment to monitor and predict the status of the drilling engineering to provide quality assurance for early warning work. In this way, it can not only improve the efficiency of early warning and monitoring of drilling engineering accidents, but also improve the quality of drilling work and promote the healthy development of drilling work.

## 3 CONCLUSION

All in all, in order to cater to the high demand for oil extraction, drilling projects need to strengthen engineering accident detection and early warning measures on the basis of ensuring work quality and efficiency, and create a safe construction environment for drilling work. At the same time, by analyzing the current situation of drilling engineering accident detection, making full use of parameter sensors, drilling tools and drilling instruments, and combining it with the expert prediction system, we can further optimize the quality of drilling engineering accident detection.

## COMPETING INTERESTS

The authors have no relevant financial or non-financial interests to disclose.

## REFERENCES

[1] Zheng Xin. Analysis of drilling engineering safety accident monitoring and early warning methods . Chemical Industry Management, 2017(18):166- 166.
[2] L. Zhang, S. Wu, W. Zheng, J. Fan. A dynamic and quantitative risk assessment method with uncertainties for offshore managed pressure drilling phases. Saf. Sci., 2018, 104: 39-54.
[3] A. Willersrud, M. Blanke, L. Imsland, A. Pavlov. Fault diagnosis of downhole drilling incidents using adaptive observers and statistical change detection. J. Process Control. 2015, 30: 90-103.
[4] J. M. Godhavn. Control requirements for automatic managed pressure drilling system. SPE Drilling Completion. 2010, 25(3): 336-345.
[5] Kinik K, Gumus F, Osayande N. A case study: first field application of fully automated kick detection and control by MPD system in Western Canada. Soc Pet Eng SPE/IADC Manag Press Drill Underbal Oper Conf Exhib. 2014:44–52.

[6] Gao Pengyue, Zhang Xinxin, Chen Han. Research and discussion on intelligent drilling engineering accident early warning system. Logging Engineering, 2016, 27(1):80-83.
[7] Kriegeskorte N. Deep neural networks: a new framework for modeling biological vision and brain information processing. Annu Rev Vis Sci. 2015:417–446.

**World Journal of Engineering Research**
**ISSN: 2959-9873**
**DOI: 10.61784/wjerv2n236**

# RESEARCH PERTAINING TO THE DIGITAL DESIGN OF ELECTRICAL WIRING SYSTEMS WITHIN POWER GENERATION FACILITIES

Rahim A. Rahman
*UM Power Energy Dedicated Advanced Centre, University of Malaya, Malaysia.*

**Abstract:** In view of the problem that the design efficiency cannot meet the design cycle in the traditional power plant design of the electrical major of power generation engineering, a wiring design method based on a digital collaborative design platform is introduced, which acquires, stores and manages the input data of the plant power, carried out load distribution and loop scheme selection, achieved a significant improvement in the quality and efficiency of factory electrical wiring design, and improved the design accuracy of power generation projects.
**Keywords:** Power generation engineering; Factory electrical wiring; Digitalization; Three-dimensional design

## 1 ANALYSIS OF CURRENT SITUATION OF POWER DESIGN OF POWER GENERATION ENGINEERING PLANTS

As the power engineering design cycle is shortening day by day and the design accuracy requirements are getting higher and higher, when the two-dimensional engineering drawing software represented by AutoCAD software is used for drawing work of factory electrical wiring design, the design efficiency has been difficult to meet the needs of the design cycle. Common design quality problems are difficult to effectively control. The three-dimensional design of power generation projects has been deepened into establishing an accurate and complete "digital power station". Incorporating the factory electrical wiring design into the three-dimensional design platform is a digital design technology that takes data connectivity as the core and is supported by multi-professional collaborative design[1]. Traditional 2D design software generally does not have multi-professional data transmission functions based on database support. Therefore, the design work is carried out in an independent manner for individual terminals. Factory electrical wiring design is carried out through the 3D design platform, which is upstream of the cable laying design in the traditional mode. The factory electrical wiring design was transferred from a two-dimensional terminal design platform to a digital collaborative design platform, which not only further deepened the design content of the "digital power station" and improved the level of design refinement, but also completely changed the design process. Achieve an overall improvement in the design efficiency of factory electrical wiring and cable laying[2].
At present, domestic and foreign power generation engineering design companies generally use two-dimensional engineering drawing software represented by AutoCAD to carry out drawing work for factory electrical wiring design. There are also some more professional design software developed based on the AutoCAD platform, such as Power Generation Software such as PROMIS.E, IPS and DLFS are widely used in engineering electrical professional design. Although two-dimensional drawing software has been used for many years in the design of electrical wiring in power generation engineering electrical majors, there are still some problems[3].

### 1.1 The Real-Time Nature of Electricity Load Data in Various Majors is Poor

Power generation engineering design is a step-by-step design process. There is a large amount of data on electrical equipment in various majors, and the data is gradually improved. At the same time, electrical equipment is limited by factors such as equipment manufacturers and mutual submission of data[4]. Electrical load data will be constantly updated and modified, and The time when the electrical load data of various majors are submitted to the electrical major is also synchronized, which results in not only increased labor costs but also an increased probability of errors for electrical designers when sorting out the electrical load data. The reason is that the electrical equipment data has been modified many times, causing work errors in the workflow transfer. During the design process, the design data cannot be updated synchronously, and the design cooperation cannot be based on a unified design platform, so the accuracy of the data cannot be guaranteed[5].

### 1.2 Factory Electrical Wiring Design and Cable Laying Design Updates are Out of Sync

Restricted by the completeness of the electrical load data of each profession, the design of factory electrical wiring cannot be carried out simultaneously with the design of each process profession. Traditional two-dimensional engineering drawing software divides the factory electrical wiring design and cable laying design into two steps. After completing the factory electrical wiring design, the cable laying design work is carried out. This not only makes the order of plant power design work in the entire engineering design cycle "solidified" in the design process, but also restricts the further improvement of design efficiency. It is impossible to realize the linkage modification of plant power

design and cable laying design. This makes It is difficult to avoid omissions and errors in electrical load and cable data during the coordination process, which will lead to design changes on site.
In addition, because the existing two-dimensional design method does not realize the data connection of all majors, there is no corresponding data management function to support it, and it is impossible to use the data completed in the cable laying design to perform complete factory power distribution system calibration calculations, and it is impossible to realize the power plant's Refined design.

## 2 DIGITAL FACTORY ELECTRICAL WIRING DESIGN PLATFORM

The digital factory electrical wiring design is based on AVEVA's process collaborative design platform (Tags). According to the factory electrical design process and the data objects involved, the design process is re-smoothed according to the design requirements, and the entire data framework is customized through the design platform. It is used to store data related to digital factory electrical design, and at the same time realizes the dynamic update of factory electrical wiring design data in the platform, and can manage the version and permissions of the data.
According to the functional requirements, logical connections, relevant specifications and other conditions of the factory electrical wiring, a reasonable loop form is selected for each load, and based on the loop wiring design, the data is transferred to the three-dimensional design environment to build cabinet and drawer models, automatically Cables are generated, and finally the cable lengths completed in the 3D design environment are returned to the wiring design for related verification.

## 3 IMPLEMENTATION OF DIGITAL FACTORY ELECTRICAL WIRING DESIGN

On the digital platform, the input data of the plant's electricity consumption is acquired, stored and managed, and at the same time, the plant's electricity load is distributed and the circuit scheme is selected. Automatically select electrical equipment parameters and cable cross-sections based on load data, and combine the data returned from cable laying to verify the cross-section selection, provide verification result reports, generate factory electrical wiring diagrams, and complete the establishment of two-way data association with digital cable laying design. .

### 3.1 Preparation Work for Digital Factory Electrical Wiring Design

In the digital factory electrical wiring design, the platform will automatically complete the selection of equipment and cables based on load data, and the selection is based on the pre-configured circuit component selection correspondence table by professional electrical designers based on relevant design specifications, design guidelines and project requirements. And the cable parameter table, import the configuration table into the three-dimensional platform according to the corresponding format. The configuration table includes a matching table of models and specifications of circuit components for motor circuits, feeder circuits and busbar contact circuits under different load power conditions. The three-dimensional platform is based on the load power entered by the process professional designer when entering the electrical load. At the same time, the electrical professional designer determines the type of the circuit as a motor circuit or feeder circuit during load distribution and circuit selection, and selects the required configuration for the circuit. components. The three-dimensional platform can automatically select the model specifications of the circuit components in the pre-entered matching table based on the load power and circuit type. As a result, it is possible to automatically select the types and parameters of motor power incoming lines, feeder power incoming lines, and busbar contact loop components. By matching with the component configuration table, it is also possible to select the cable cross-section for the circuit.

### 3.2 Load Distribution and Circuit Assembly

Through the operation interface of the platform, the load and bus data stored in the database are read, and the unallocated loads and buses are associated with each other. Before the correlation, the circuit is selected for each load through the function of selecting the electrical load circuit wiring element. element. The platform can automatically select the model specifications of the circuit components in the pre-entered matching table based on the load power and circuit type.
Based on the load of the selected circuit components, the platform will automatically determine the size of the space it occupies, and use this data information as the basis for circuit assembly.

#### *3.2.1 Load distribution*

The purpose of load distribution is the process of allocating it to reasonable bus sections based on the power of the load itself and the corresponding technical parameters. The distribution principle is determined according to the relevant design specifications, and the digital platform realizes the establishment of the power supply relationship between the recorded load and the busbar [3].
Before load distribution, typical load circuit configuration needs to be performed on the platform. According to the technical parameters of the load and referring to relevant design specifications and design guidelines, the electrical component configuration of the load loop can be determined on the platform loop configuration interface. Typical circuit configurations are divided into three categories: load type (feeder circuit, motor circuit, motor circuit with differential protection), typical circuit configuration component selection (circuit breaker, fuse, contactor, current

transformer, zero sequence current transformer, Overvoltage protector, thermal relay, grounding switch, zero sequence current transformer), local equipment (iron case switch, frequency converter, local controller, magnetic starter). The load type and circuit scheme are required, and local equipment is optional. All loads in the project need to be distributed to reasonable bus sections before circuit grouping can be carried out.

#### *3.2.2 Circuit panel*

Factory electrical wiring needs to express the number of panels under each bus section, the number and type of circuits in the panels, the installation controls and drawer numbers of the drawers corresponding to each circuit, the circuit configuration of the circuits corresponding to each drawer, and the number of each configuration component. Model parameters, as well as the cable code, cable model and cable specification corresponding to the circuit.

When the circuit is assembled, the digital factory power design platform will automatically match the component parameters and models based on the typical circuit electrical component selection scheme set in the background database in advance. The first condition for automatic matching is the load type, and the second condition is the load rated power. Based on the above two conditions and the electrical components selected for the load circuit during load distribution, the model and parameters of the selected components can be determined, the cable model and specifications that meet the current circuit can be determined, and the size information of the drawer corresponding to the current circuit can also be obtained .

The total volume of drawers that each panel cabinet can accommodate is limited. When each circuit is assembled, the required drawer size can be automatically calculated based on the typical circuit matching relationship. Before placing each circuit into the cabinet, the software automatically calculates whether the remaining space in the current cabinet can accommodate the drawers required for the selected circuit.

There are two situations for panel grouping: one is to single-select or multiple-select the load under the current bus to directly group the panel, and the other is to insert the selected circuit into an existing panel cabinet. In both cases, the software will automatically calculate whether the space requirements can be met before completing the disk grouping, and the system will automatically prompt if the requirements cannot be met.

### 3.3 Cable Data Transmission and Verification

#### *3.3.1 Cable data transfer*

The core of the factory power design platform is data transmission, which is reflected in the platform automatically selecting electrical equipment parameters and also selecting the cable cross-section for the loop. In the 3D model design environment, cable information in the wiring design can be automatically obtained: cable codes, starting and terminal equipment codes, cable model sections, etc., as the initial cable inventory for cable laying design.

First, check whether the starting and terminal equipment of the cable exist in the 3D model design environment through the unique code of the equipment (KKS code). Secondly, check whether the cable model specifications have matching items in the model database. When the above two conditions are met, the cable data model is automatically generated in the three-dimensional design environment. If the wiring diagram is modified in the middle and later stages, the software can also automatically compare whether the cable information in the 3D design environment is consistent with the wiring design. The user can decide whether to modify the cable information in the 3D design.

For cables that have been laid and designed in the 3D model environment, the length can be returned to the wiring design environment for relevant verification calculations.

#### *3.3.2 Related check calculations*

After the plant power design platform obtains the cable length from the model design environment, it combines the pre-entered calculation parameters of the feed network, transformer, and motor with the "cable characteristic matching table" in the database. Through the above parameters, as well as the load and busbar, busbar and The connection relationship between busbars is based on DL/T5153 - 2014 "Technical Regulations for Power Design of Thermal Power Plants". The digital platform can automatically calculate the effective value of single-phase short-circuit current at the end of the cable, the effective value of three-phase short-circuit current and the terminal voltage loss. .

After the verification calculation is completed, the electrical designer will judge whether the design requirements are met based on the results. If the verification calculation results do not meet the design requirements, the design platform will return the information to the load distribution and panel assembly, reselect the cables, and then complete the cable laying through data transmission. The cable length is returned to the factory electrical wiring design, and the verification calculation is performed again until the verification results meet the design requirements.

## 4 THE FINISHED PRODUCT OF ELECTRICAL WIRING DESIGN FOR DIGITAL FACTORY

### 4.1 Factory Electrical Wiring Diagram

After the busbar wiring design is completed, it is verified through relevant calibration calculations to meet the design requirements. Based on the results of load distribution and circuit grouping, the platform's own report tool can be used to generate a busbar-based wiring diagram. The report format is customized based on the finished product model designed by the electrical wiring diagram of the electrical professional factory. The wiring diagram includes: switch cabinet KKS code, primary configuration diagram in the cabinet, circuit breaker information, fuse information, contactor information, current transformer information, voltage transformer information, overvoltage protector information, grounding switch information, zero sequence current Transformer information, cable information (KKS

code, model, number of roots, core number, cross-section), terminal load/power supply information (name, KKS code, rated capacity, rated current, overvoltage protector, current transformer), secondary Picture number, etc.

### 4.2 Cable Inventory

After the cable laying is completed in the 3D model design environment, the cable length, cable detailed path, buried pipe specifications and length information can be obtained in the factory power design platform. By customizing reports, cable inventories can be generated with one click. The cable inventory includes: cable number, buried pipe specifications, buried pipe length, cable specifications, cable starting end code, cable starting end description, cable terminal code, cable terminal description, cable length, cable laying path and other information.

### 4.3 Board Layout Diagram

According to the circuit group information of a certain panel cabinet in the Tags wiring diagram, that is, the number of drawers in the cabinet and the space occupied by each drawer, in the three-dimensional modeling module Equipment, the drawers of the cabinet can be completed with one-click operation. Model creation means that the cabinet is divided into a specified number of drawer models and automatically named. Then through the drawing module, the panel layout can be completed.

## 5 CONCLUSION

The problem of inconsistency between wiring design and cable design caused by modification of process data; by pre-setting the typical loop component selection table, quickly select loop components and improve design efficiency; automatically calculate short-circuit current and voltage drop to reduce the probability of errors; can Draw uniform wiring diagrams and cable inventories based on customized templates.

Factory electrical wiring is one of the important contents of the electrical professional design of power generation projects. The design of factory electrical wiring is incorporated into the three-dimensional collaborative design platform to realize the data connection between the electrical equipment of various process professions and the electrical professional power distribution equipment and cables. It can break through the constraints of traditional two-dimensional design on the overall design progress of the electrical major, and is expected to advance the overall design progress of the relatively lagging electrical major and improve design efficiency. The digital factory electrical wiring design platform not only manages load data, but also includes design products such as factory electrical wiring diagrams after verification and calculation, as well as seamless connection with cable laying work on the three-dimensional platform, promoting complete and accurate design. The process of refined design of the three-dimensional "digital power station".

## COMPETING INTERESTS

The authors have no relevant financial or non-financial interests to disclose.

## REFERENCES

[1] Song Kang. A brief discussion on how to improve the power design efficiency of power plants. Science and Technology Information Development and Economics, 2010, 20(3): 227-228.

[2] A. Chatterjee, A. Keyhani, D. Kapoor. Identification of photovoltaic source models. IEEE Trans. Energy Convers. 2011, 26(3): 883-889.

[3] Liu Sijia, Huang Haicai, Jia Liying. Research on power wiring scheme for large thermal power plants. Power Grid and Clean Energy, 2013, 29(10):37-41.

[4] J. A. Gow, C. D. Manning. Development of a photovoltaic array model for use in power-electronics simulation studies. IEE Proc. Electric Power Applicat. 1999, 146(2): 193-200.

[5] Chen Haihua. Selection of voltage level for 1000 MW unit high-voltage plant power system . North China Electric Power Technology, 2013(4):25-28.

**World Journal of Engineering Research**
**ISSN: 2959-9873**
**DOI: 10.61784/wjerv2n237**

# RISKS AND COUNTERMEASURES DURING THE DISASSEMBLY AND INSTALLATION OF THE WELL TEAM

Seunghee Oh
*Department of Safety Engineering, Incheon National University, Korea.*

**Abstract:** In recent years, the application of the latest researched equipment installation technology has promoted the development of related industries to a large extent. However, there are still some problems in the application of domestic well team disassembly and installation technology, such as management issues, quality issues, or dangers that arise during project implementation, all of which we are faced with. In order to further improve the current situation, it is necessary to continuously improve the process level, and at the same time, constantly standardize the control and management system, etc., and improve various problems that arise during the disassembly and installation of the well team through improvements in different aspects. With the continuous application of information technology and the increasing emphasis on technical safety in all countries in the world, it is necessary to further improve the application of intelligent, digital and information technology in the installation and construction of well teams. This can not only reduce labor costs, To a certain extent, it can also improve the installation efficiency, further improve the economic benefit level of the industry, and further promote the strong development of the industry.
**Keywords:** Well team construction; Risk response; Management system

## 1 CHARACTERISTICS OF THE INSTALLATION, CONSTRUCTION AND DISASSEMBLY PROCESS OF THE WELL TEAM

With the continuous development and progress of the times, especially after entering the 21st century, under the influence of the tide of information technology, the development of various industries in our country has made great progress. Using modern technology, many industries have gradually got rid of the traditional industry[1]. On the other hand, our country's trade exchanges with some foreign countries have gradually increased, and learning from foreign advanced technological experience has also had a great impact on the development of various industries in our country. At present, the development of well team installation and construction in our country has also made great progress. The level of construction technology is improving day by day[2]. At the same time, the control and management of well team installation and construction are also constantly updated and improved. After the development and improvement in recent years, it can be seen that , the internal management level of the well team has been improved, but there are also some problems, such as the overall quality of the installation personnel is not high, the control management system is not standardized enough, etc., which need to be promoted by improving the technical level or cultivating more technical talents. The continuous development of this industry in our country[3].

### 1.1 High Risk

Well team installation and construction can not only ensure normal production, but also have a significant impact on the actual level of the entire life, and are widely used. Therefore, the installation quality of the well team has a great role in promoting the development of our country's economic level and is cost-effective. At the same time, the investment in the well team disassembly project is also risky. When applying it, the entire operation must be taken into consideration. The environment and the physical condition of the well team members enable the well team leader to make more accurate predictions for different situations at work[4-5].

### 1.2 High Technical Content

Installation is the key to improving the implementation of the entire well team. At the same time, it has a great impact and the technical requirements will be very high. Compared with the traditional installation and production, the installation technology content is significantly improved. If the entire well team's installation technology is not Innovation and improvement will seriously affect the entire production process of the project[6]. Therefore, in practical applications, there are still some obstacles to the well team installation project, so it is necessary to continuously increase the technical investment in installation and continue to conduct learning and research so that it can better serve socialized mass production and further enhance our country's economic level.

## 2 WELL TEAM INSTALLATION AND DISASSEMBLY MANAGEMENT MEASURES

### 2.1 Do a Good Job in Checking the Installation and Disassembly of Equipment in Every Link

By introducing the analysis of the characteristics of well team installation, it can be concluded that its main characteristics are high risk and high technical content, so its application requirements are also very high. How to better improve the application effect of well team installation and disassembly requires strengthening its installation management and improving its actual application effect by inspecting the installation equipment in every link. On the one hand, we must do a good job in inspecting the installation in the market we are facing to ensure its quality in production; on the other hand, we must improve the management of the well team itself. Next, we will introduce the standard internal management system of the well team.

### 2.2 Standardize the Internal Management System of the Well Team

The completion stage of the well team installation and disassembly project is the most critical part of the entire construction process. Acceptance of the completed work can prevent unnecessary quality problems during future use and ensure the service life of the operation. The main improvement method for the problem of unclear target responsibilities in actual installations is to focus on building a cost target indicator system and a cost responsibility system with unified rights and responsibilities. Only after the responsibilities are specifically clarified can the well team improve management. Only with a fixed direction to pursue can we build a more stable management target indicator system. In the process of improving the well team management system, in addition to mobilizing employees, it also lies in the guidance of well team leaders to make correct decisions.

## 3 METHODS FOR LIFTING WELL TEAM INSTALLATION AND DISASSEMBLY PROJECTS

### 3.1 Improve its Sewage Treatment Technology

At present, a prominent problem in the application of well team installation is the emission of pollutants, which causes environmental pollution. Therefore, in future applications, we must continue to improve pollution control issues and upgrade pollution control technology. This will create greater social value, achieve higher social benefits, and adhere to our country's sustainable development path. Make a contribution to global environmental protection.

### 3.2 Strengthen the Application of Intelligent Technology

The 21st century is the information age, and intelligence has been applied in the production and development of many industries. In the design and management of well team installation, we must also improve the application of informatization and intelligent technology, and actively learn the application of foreign advanced technologies. Through the application of intelligent technology in actual installation design, the difficulty of control and management of well team disassembly technology can be reduced, human misoperation can be reduced, and the orderly development of equipment and packaging technology can be improved.

### 3.3 Implement a Performance Point Assessment System to Improve Employees' Work Enthusiasm

The employees of an enterprise are the core element for the operation of the entire enterprise. In addition to funds, employees are the factor with the greatest influence on the enterprise. They will not only affect the overall operation ability of the enterprise, but also affect the profit of the enterprise. Therefore, the same is true for the well team. Its main leaders must improve and standardize the employee salary system. On the basis of more work, more gain, less work, less gain, a performance point assessment system must also be implemented, that is, for employees to make suggestions incentive system. For example, you can stipulate that employees who work overtime will receive different bonuses. At the same time, for some innovative and technical talents within the well team, as long as they have contributed to the well team, they should be rewarded. They gave rewards to encourage the well team employees to devote themselves to work with greater enthusiasm, and made plans for the company, which on the other hand ensured the safety of the well team's construction.

## 4 CONCLUSION

At present, there are still some problems in the domestic electrical construction technology and control management of electromechanical installation projects. But in general, installation workers are required to have high professionalism, because good workmanship is required in every aspect of installation. Therefore, not only the management personnel must be paid attention to, but also the installers must be given sufficient attention. Concern in this regard can be achieved by establishing a performance point assessment system or a certain incentive system to enhance staff's enthusiasm for work input. No matter what industry it is, its development must be based on continuous innovation and improvement strategies.

## COMPETING INTERESTS

The authors have no relevant financial or non-financial interests to disclose.

## REFERENCES

[1] Wang Jianxue. Drilling Engineering. Beijing: Petroleum Industry Press, 2008.
[2] Go, S. A study on quantifying risk index by performing risk assessment of building construction work, Research Report, Korea Occupational Safety and Health Research Institute, Korea. 2003.
[3] Fan Hua, Wei Longchao. Summary of maintenance methods and practices of commonly used electrical equipment in drilling teams. Technology to Get Rich Guide, 2012(05).
[4] Lee, C. The investigation of recent three year construction projects by the type of works and accidents, Research Report, Korea Occupational Safety and Health Research Institute, Korea. 2010.
[5] Stewart, R.A., Mohamed, S. Evaluating web-based project information management in construction: Capturing the long-term value creation process. Automation Construction. 2004, 13(4): 469–473.
[6] Lim, J., Han, K., Kim, S. A study of client role for safety management at construction sites. Korea Institute of Building Construction. 2008, 8(5): 75–83.

**World Journal of Engineering Research**
**ISSN: 2959-9873**
**DOI:10.61784/wjerv2n237**

# DISCUSSION ON A NEW MODEL OF WATER AND ELECTRICITY GENERAL CONTRACTING MANAGEMENT BASED ON TECHNOLOGY LEADERSHIP AND STANDARDS FIRST

Ellen Ortiz
*School of Engineering and Physical Sciences, University of New Hampshire, Durham, NH, USA.*

**Abstract:** With the development of basinization and scale of hydropower project construction, the adoption of the EPC general contracting model for large-scale hydropower project construction is an innovation in the construction model, and it also poses challenges to the general contracting management level of hydropower projects. This article adopts the practice of general contracting management of Yangfanggou Hydropower Station design and construction, adopts the model of a close alliance, strengthens technological innovation and optimization through the integration of design and construction, improves the level of engineering technology, and further improves engineering risk control capabilities and efficiency, in terms of quality and Standardization takes precedence in safe and civilized construction management, and informatization is implemented in the entire process of project construction to improve the informatization level of project construction and operation management, which can provide reference for similar general contracting projects of hydropower projects.
**Keywords:** Technology integration; Standardization; Unformatization; General contracting; Yangfanggou Hydropower Station

## 1 PROJECT OVERVIEW

Yangfanggou Hydropower Station is located in Muli County, Liangshan Prefecture, Sichuan Province in the middle reaches of the Yalong River. It is the sixth-level hydropower station in the planned "one reservoir and seven levels" of this river section. The normal water storage level of the power station is 2094m, the corresponding storage capacity is 455.8 million m3, and the installed capacity is 1500MW. The engineering hub consists of major buildings such as a concrete double-curved arch dam, flood discharge and energy dissipation buildings, and a water diversion and power generation system.

Yangfanggou Hydropower Station is my country's first large-scale hydropower project with a million-kilowatt capacity constructed using the design and construction general contracting model. It was built by a consortium composed of China Water Conservancy and Hydropower No. 7 Engineering Co., Ltd. and PowerChina East China Survey and Design Institute Co., Ltd. The project started in January 2016, and the river closure was completed ahead of schedule on November 11, 2016. It is planned that the first unit will generate power in November 2021, and the project will be completed in June 2023.

In more than two years of exploration and practice, Yangfanggou General Contracting Department has fully integrated design and construction technology, focused on design innovation and optimization, put standardization first in quality and safety management, fully utilized the role of informatization in construction management, and provided Useful exploration has been made in innovating the general contracting management of design and construction of large hydropower stations.

## 2 INTEGRATION OF DESIGN AND CONSTRUCTION TECHNOLOGY

### 2.1 Ensure Supply of Design Products

The design leader is not only the first person in charge of the design team, but also a team member of the general contracting department. He participates in project management and establishes a platform for good communication between design and construction. As a functional department of the general contracting department, the design management department works under the leadership of the general contracting department, making it easier and faster to contact and communicate with other functional departments[1]. As a work area of the general contracting department, the design representative office closely cooperates with the construction and gives full play to the design skills. Technology leads the way and serves on-site construction.

Since design drawings require approval by the design supervisor before they can be used for construction, the arrangement of the design schedule plays a vital role in the progress of the entire project. The design department hosts monthly meetings, with relevant departments and work areas participating. Based on the annual plan, they discuss the

construction drawing supply plan within the next three months, and the 3-month drawing supply plan will be included in the design department Daily work assessment scope[2]. For projects that are temporarily added or constructed in advance, the design unit must be notified in advance to allow reasonable design time. During the design process of construction drawings for key line projects, the designer communicates with each work area in advance the main content and relevant details in the drawings. The work area can prepare for construction in advance, which will help shorten the construction cycle and ensure the achievement of progress goals.

In the case that some working surfaces fail to meet the progress requirements due to various factors during the construction process, the designer actively participates in the progress analysis and adjustment of the project, and ensures the progress requirements through design changes, construction method changes and other measures approved by the owner.

### 2.2 The Implementation of Design Intentions is Further Improved

Under the EPC model, design and construction are closely integrated. The general contracting department has established a mutual signing system for design and construction technical documents. All design drawings are countersigned by the general contracting technical management department and relevant work areas before issuance, and the design plan and on-site construction may exist Conflict issues and problems that are inconvenient for construction should be resolved before the drawings are submitted to the supervisor for review to improve the implementability of the design plan[3]. Similarly, the layout of construction branch tunnels, construction plan measures, etc. are also countersigned by the designer to ensure that the temporary construction layout and construction measures can better meet the overall structural requirements of the project and make the layout more reasonable. The design and construction are fully reflected in the determination of technical documents. Integrated advantages.

In terms of on-site design modifications, in response to changes in on-site geological conditions and construction conditions, the designer keeps abreast of changes in on-site conditions, understands the needs during the construction process, and more actively participates in on-site design modifications to address the urgent needs of the project and proactively create new solutions for the construction. favorable conditions.

### 2.3 Further Improve Project Risk Control Capabilities and Efficiency

Through the mutual signing system of design and construction technical documents, the design plan and construction measures can truly adapt to the actual site conditions and equipment capabilities, making them more effective and operable. Major technical plans adopt a special discussion system, and scientific decisions on technical plans are made through special discussions. Full disclosure of construction drawings and construction technical requirements step by step, coupled with sufficient daily communication, enables the construction team to thoroughly understand the design intent and master the key points of quality and safety control, which is conducive to better control during construction[4].

Establish an integrated working mechanism for dynamic design and construction, closely integrate design with geology, construction, and monitoring, and adopt the concept of "dynamic design and construction" to optimize excavation and support parameters in a timely manner to guide safe and rapid construction. Technical quality risk management and control meetings are organized every week, and countermeasures are proposed based on the quality, safety and risks discovered through geological analysis, safety monitoring, scientific research and on-site supervision in the design, to improve the project risk management and control capabilities and efficiency, and to effectively ensure the technical safety of the project. construction.

## 3 TECHNOLOGICAL INNOVATION AND OPTIMIZATION

### 3.1 Pursue Optimal Engineering Value and Overall Project Benefits

Design is the leader in project construction. It is necessary to rationally design hub buildings and electromechanical equipment under specific hydrological, geological and other conditions to meet various requirements for power station operation. Under the EPC model, the contract is a lump sum model, and the design unit plays a more prominent role in project construction and general contract performance.

Under the EPC model, all parties involved in the construction have different focuses due to their own responsibilities and requirements. The owner will put forward high-quality and high-standard requirements for the project without changing the total price; the supervisor will conduct a multi-dimensional review of the functionality, safety, investment, etc. of the design results; the general contractor will control the cost while ensuring quality and safety. Require[5]. This requires the design unit to have more comprehensive and profound technical capabilities and the coordination and communication ability to handle complex relationships. Excellent design must pursue the optimal engineering value and overall project benefits, and must comprehensively balance the optimal realization of multiple goals such as project safety, quality, schedule, operation management, and life cycle costs.

### 3.2 The Concept of Quota Design Runs Through The Entire Design Process

Design units must always pay attention to the impact of the solution on cost during the product design process. Designers must be familiar with the contract's functional requirements, contract project and project quantity requirements. Each product must be compared with the contract price, and the design limit shall be Put it into practice[6]. The General Contracting Department gives full play to its design technology advantages, and while ensuring that the functions of each part of the project meet the contract requirements and facilitates operation and maintenance, it actively carries out technological innovation and design optimization through the integration of design and construction to enhance the value of the project. Actively think about design optimization, strictly control changes through refined design, and ensure that the total investment is within the limit of the total contract price.

From 2016 to 2017, 23 major optimization items were completed and passed the review, such as the optimization of the arch dam foundation surface and in-depth research on the body structure, in-depth research on flood discharge and energy dissipation facilities, and the optimization of the treatment plan for the collapse and slope accumulation, etc., saving project investment. More than 70 million yuan. Complete construction optimization 10 For items, construction optimization is mainly to improve construction conditions, reduce construction safety risks, improve construction efficiency or ensure construction progress, etc., which is basically the same as the bidding investment[7].

## 4 STANDARDIZED MANAGEMENT FIRST

Standardization is the establishment of common, reusable rules for repetitive matters in management activities. It includes the process of formulating, publishing and implementing standards. The General Contracting Department comprehensively implements standardization of quality, safety, construction and material management.

### 4.1 Quality Management Standardization

In accordance with the contract requirements, the general contracting department strengthens internal self-discipline management, and consciously controls project quality during the front-line construction process, so that project quality is more guaranteed. The General Contracting Department actively promotes quality standardization operations. Based on the progress of the project, it formulates standardized documents for main construction processes, and prepares quality process standardization for slope excavation, cavern excavation, mortar anchors, shotcrete, steel bar formwork, and anchor cable construction. Manual; in order to let the standardization results go deep into the front line and be implemented by people, the general contracting project department subdivided the construction process documents into three categories: "construction process standards, construction process manuals, and construction quality understanding cards" for personnel at different levels and different management departments. levels, respectively provided for use by project managers, on-site quality inspectors, and front-line operating workers, so that the key points are highlighted, easy to understand, and convenient for on-site operations. Carry out hierarchical publicity and implementation training on process standardization, fully covering on-site quality management, engineering technology, construction management and other levels of personnel. On-site construction strictly follows standardization requirements, which greatly improves the standardized construction awareness of on-site personnel at all levels and effectively promotes the project Improvement of quality.

The Yangfanggou General Contracting Department has established the first quality management standard demonstration exhibition hall in the domestic hydropower industry, which comprehensively displays quality management system documents, civil and mechanical and electrical construction process quality control standards and standard process exhibits to provide on-site training and benchmarking construction for the project. A dedicated place. By the end of 2017, this project had completed a total of 3,682 unit inspections, with a pass rate of 100% and an excellent and good rate of 96.4% (contract requirement of 85%).

### 4.2 Safety Management Standardization

Under the general contracting model, the safety management responsibility of the project entity is the responsibility of the general contractor who is directly responsible for production management, and the general contractor's responsibilities are more clear. The general contracting department actively and orderly promotes safety management work, taking advantage of the integration of design and construction in the investigation and rectification of hidden dangers and the planning of special safety measures, and based on the actual situation of the general contracting project, established "one manual", "two plans" and "seven The main line of security management of "account" is implemented more effectively. A safety standardized atlas has been compiled and distributed to each work area, with unified standards for pipeline layout, adjacent protection, safety warnings, temporary facility layout, etc., and the image of safe and civilized construction has been steadily improved.

The first safety facility experience hall in the Yalong River Basin was established to simulate emergency rescue, falling from high altitude, object hitting, electric shock and fire, adjacent instability and other emergency situations, making safety education and training routine and comprehensively improving safety education. In terms of construction, the

general contracting department unified the planning and layout of temporary construction facilities. Temporary construction factories and enterprises such as steel bar factories, formwork factories, and comprehensive warehouses have unified standards, and random private construction is strictly prohibited. Strictly organize and implement production safety standards to ensure on-site production safety since entering the site. Yangfanggou Hydropower Station passed the first-level assessment of power safety production standardization in the first year after the project started.

## 5 THE WHOLE PROCESS OF PROJECT CONSTRUCTION AND ALL-ROUND INFORMATION MANAGEMENT

The application of informatization in hydropower projects has become a major trend. Efforts to promote the informatization construction and management of hydropower projects will help improve the construction quality and management efficiency of hydropower projects. Under the traditional model, design, construction, and operation and maintenance are separated in the industrial chain, with poor coordination capabilities and the failure to effectively circulate data at each stage, which has greatly hindered the development of information technology. The general contracting model can break industrial fragmentation and realize real-time sharing of information. The Yangfanggou General Contracting Department has established an information platform of “one OA platform + one BIM system”, which is of great significance for improving project management efficiency[8].

### 5.1 Comprehensive Office OA System

The comprehensive office OA system of Yangfanggou General Contracting Department is based on a new management structure and ideas, covering system portal, personal office, information release, comprehensive office, human resources management, correspondence management, drawing management, procurement management, system management, mobile office and other subsystem modules to realize collaborative management and control and mobile office of the general contracting project department. The comprehensive office OA system is mainly for the release and sharing of internal organizational information of the general contracting project department. Each module operates independently according to the division of labor and authority of the department. At present, more than 20 subsystems and modules related to daily management, office, and services are running normally, providing strong information technology means and support for the development of various work on the project site, and greatly improving work efficiency.

### 5.2 Design and Construction Bim Management System

The General Contracting Department established a BIM management system for the design and construction of the Yangfanggou Hydropower Station. Taking engineering big data management and control as the entry point, the general contracting department used digital means and BIM technology to comprehensively manage and control the project construction progress, quality, investment, and safety information. The functions of the BIM management system The modules include: comprehensive display, design management, quality management, progress investment, video surveillance, safety monitoring, water condition forecasting, intelligent grouting, concrete temperature control, etc. During the construction period of the project, the general contracting department, supervisors and owners all use the BIM management system for construction management, which can effectively realize the visual intelligent management of the project and improve the informatization level of project construction and operation management. The BIM management system uses information technology to collect and save project-related information from the beginning of the project, providing a foundation for the management of the entire project life cycle.

### 5.3 Quality And Safety Management App

In order to facilitate access to information and quickly deal with quality and safety issues discovered on site, the General Contracting Department developed the "Quality Management APP" and "Safety Management APP". The quality management APP includes functional modules such as quality issue tracking, quality information statistics, quality assessment application, and system standard documents, allowing project participating unit personnel to fully understand project quality management information and quickly handle quality issues on their personal mobile terminals. Improve quality management efficiency and enhance quality management transparency. The safety management APP includes functional modules such as risk identification and assessment, risk investigation and governance, risk process management and control, and system standard documents. It allows personnel from participating units to view the safety risks and control measures of each work surface on their personal mobile terminals, and evaluate the safety risks and control measures found on site. Safety risks are quickly reported, rectified and closed to improve safety management efficiency.

This project is one of the first batch of pilot projects of the State Grid's pumped hydro energy storage project. The smooth performance of the contract is of great significance to State Grid Co., Ltd., Power Construction Corporation of

China, and the entire pumped hydro energy storage engineering field. The project has just started construction. How to improve the performance model of EPC projects is still a research topic with a long way to go. It is also necessary to continuously improve and summarize the results of project performance and problems that arise during the process to provide more experience for the development of the EPC model of engineering construction.

## 6 CONCLUSION

The engineering EPC general contracting model is the development direction of construction project management. The core of EPC general contracting is the integration of design and construction. The Yangfanggou Hydropower Station adopts the EPC construction management model, which is the first time that my country's large-scale hydropower projects with a million-kilowatt capacity are constructed using the EPC construction management model. It is a major change in the concepts and methods of hydropower development, traditional construction systems and management models under my country's new normal. Innovation.

Through the integration of design and construction technology, Yangfanggou General Contracting Department strengthened technological innovation and optimization, improved the level of engineering technology, and further improved the implementation of design intentions and the level of engineering risk control. Standardization takes precedence in quality and safety and civilized construction management, which greatly improves the standardized construction awareness of personnel at all levels on site, ensures the quality of the project, and enhances the image of safe and civilized construction of the project; during the construction period, all parties involved in the project use the BIM management system. Construction management implements informatization in the entire process of project construction, comprehensively improving the informatization level and management efficiency of project construction. The practical exploration of general contracting management of Yangfanggou Hydropower Station can provide reference for similar projects.

## COMPETING INTERESTS

The authors have no relevant financial or non-financial interests to disclose.

## REFERENCES

[1] Qu Feiyu. International project general contracting model and current situation of development in china. Market Weekly, 2008, (10): 72-75.

[2] Hu Deyin. Lecture on Modern EPC Engineering Project Management. Chemical Engineering Design, 2003, 13(3): 41-45.

[3] Wisser, D., Fekete, B. M., Vörösmarty, C. J., Schumann, A. H. Reconstructing 20th century global hydrography: a contribution to the Global Terrestrial Network- Hydrology (GTN-H). Hydrol. Earth Syst. Sci., 2010, (14): 1–24.

[4] Liu, L., Hejazi, M., Patel, P., Kyle, P., Davies, E., Zhou, Y., Clark, L., Edmonds, J. Water demands for electricity generation in the US: Modeling different scenarios for the water-energy nexus. Technol. Forecast. Soc. Chang. 2015, 94, 318–334.

[5] Flörke, M., Kynast, E., Bärlund, I., Eisner, S., Wimmer, F., Alcamo, J. Domestic and industrial water uses of the past 60 years as a mirror of socio-economic development: A global simulation study. Glob. Environ. Chang. 2013, 23, 144–156.

[6] Macknick, J., Newmark, R., Heath, G., Hallett, K.C. Operational water consumption and withdrawal factors for electricity generating technologies: A review of existing literature. Environ. Res. Lett. 2012, 7, 045802.

[7] Lin, L., Chen, Y.D. Evaluation of Future Water Use for Electricity Generation under Different Energy Development Scenarios in China. Sustainability 2018, 10, 30.

[8] Cooley, H., Fulton, J., Gleick, P.H., Ross, N., Luu, P. Water for Energy: Future Water Needs for Electricity in the Intermountain West, Pacific Institute: Oakland, CA, USA, 2011.

**World Journal of Engineering Research**
**ISSN: 2959-9873**
**DOI: 10.61784/wjer3001**

# OVERALL FLOOR FLATNESS CONTROL TECHNOLOGY FOR ULTRA-LONG AND ULTRA-LARGE EXHIBITION HALLS

ZhiChao Zeng[1,2], XiaoJu Zhang[1,2,*], XuanZhong Luo[1,2], ZhiYuan Zhang[1,2], ZhenJie Tan[1,2]
[1]*China Construction Fourth Engineering Bureau Co., Ltd. Guangzhou, Guangdong 510000, China;*
[2]*China Construction Fourth Engineering Bureau Sixth Construction Co., Ltd. Hefei, Anhui 230000, China.*
*Corresponding Author: XiaoJu Zhang, Email: 19822660870@163.com*

**Abstract:** With the continuous development of modern construction technology, the demand for the construction of super-long and super-large exhibition halls is increasing. The flatness of the exhibition hall floor directly affects the display effect and usage function. Therefore, higher requirements are put forward for the control technology of floor flatness. This paper studies the flatness control technology in the construction process of super-long and super-large exhibition hall floors, and studies a customized special adjustment bracket to fix the floor armor seam and cooperate with laser or optical level to accurately measure and control the floor flatness.
**Keywords:** Super-long and super-large exhibition hall; Floor flatness; Control technology; Construction process

## INTRODUCTION

Due to their unique spatial requirements, ultra-long and ultra-large exhibition halls have strict requirements on the flatness of the floor. The flatness of the floor is not only related to the beauty of the exhibition hall, but also directly affects the display effect of the exhibits and the visitor's experience. Therefore, the study of the control technology of the flatness of the floor of ultra-long and ultra-large exhibition halls has important practical significance [1-2].

## 1 PROJECT OVERVIEW

The first phase of the Hangzhou Convention and Exhibition Center project covers an area of about 360,000 square meters, with a total construction area of 643,200 square meters, a ground construction area of 423,500 square meters, and an underground construction area of 219,700 square meters. It consists of a ground garage and 8 exhibition halls, 2 login halls, a central corridor and some outdoor exhibition areas. The underground project is a reinforced concrete frame structure, and the ground structure is a large-span steel structure.

## 2 CONSTRUCTION METHODS

In actual construction, different methods need to be applied in combination with actual conditions and engineering construction experience. For example: plane overall partition construction method, split-seam skipping construction method. The width of the split-joint jump-bin is 6 m, and the smallest interlayer unit is 6 m×6 m or 4 m×6 m. In order to prevent local settlement cracks and surface temperature cracks in the floor, the compaction degree of the concrete surface layer is controlled first, and then a double-layer bidirectional steel wire mesh is configured in the floor. The bottom layer is HRB400 grade 5mm diameter steel wire mesh with a spacing of 200mm, and the concrete protective layer thickness is 45mm. The upper layer is HRB400 grade 2mm diameter steel wire mesh with a spacing of 200mm and a concrete protective layer thickness of 30mm. The bottom layer of steel wire mesh is laid in sections and overlapped at the jump-bin casting joint to prevent local uneven settlement and deformation of the ground. The upper layer is continuously overlapped in the unit block, and the separation joints are disconnected to prevent cracking of the ground. The concrete pouring adopts the rail leveling strip jump-bin method for construction [3].

## 3 CONSTRUCTION TECHNOLOGY

### 3.1 Guide Rail

Guide rails are generally made of 50×20 (wide) channel steel or 50×25 square steel pipe. The width should be narrower, otherwise the steel bar protective layer will be too thick. The spacing between the guide rails should be determined according to the width of the concrete to be poured, but it should generally be less than 4 meters; the guide rails are fixed with a tripod with a Φ12 screw rod, and the tripod spacing should be less than 1000 ㎜; the guide rail surface level is controlled and measured with a level. The guide rail is adjusted by two nuts that fix the channel steel with a Φ12 screw rod. During the construction process, the level of the guide rail should be checked once in a while for timely adjustment.

### 3.2 Concrete Pouring and Vibration

Before concrete construction, the floor concrete mix ratio is designed: according to the local material characteristics, working conditions, and weather conditions in Hangzhou, the material manufacturer that provides the overall floor system pre-concrete trial mixing in a fixed laboratory until the trial mix concrete meets the requirements, and then submitted to the mixing station for processing according to the trial mix requirements.
Just like Figure 1, the trial mix of concrete for flooring added a multi-phase composite material - steel fiber: the content of steel fiber per kilogram was about 4,600 fibers, and 10-15 kilograms per cubic meter of concrete. The steel fiber distribution density was extremely high, which fully changed the brittleness of concrete, improved the toughness and ductility of the concrete slab, and increased the allowable bending deflection of the slab. The steel fiber was distributed in three dimensions in the concrete from the bottom of the floor to the entire cross-section, which can reinforce the concrete from all directions. The extremely high density can effectively improve the bonding and bite force between the steel fiber and the aggregate, improve the floor's anti-cracking ability, improve the hollowing phenomenon, and effectively ensure the integrity of the floor [4].

**Figure 1** Concrete Pouring

### 3.3 Rolling with a Drum

The drum is made of Φ150 steel pipe. The drum is dragged back and forth along the guide rail to achieve the purpose of preliminary leveling. After grinding with a disc machine to produce slurry, it is rolled flat with a drum.

### 3.4 Grinding with a Disc Machine

When the concrete is about to set, that is, when the slump of the concrete basically disappears, the concrete is ground with a disc machine to make the concrete surface produce slurry again.

### 3.5 Scraping with an Aluminum Alloy Ruler

Scraping the concrete surface with an aluminum alloy ruler is an important process to ensure that the surface flatness of the concrete meets the quality requirements. The aluminum alloy ruler should be selected with a large cross-section with high rigidity and not easy to deform, and the length should be 4m to 6m long; after the disc machine grinds the concrete surface to produce slurry, use the aluminum alloy ruler with the channel steel as the guide rail to rotate and scrape the concrete in any direction. After the guide rail is removed and slurry is added, it is scraped flat with an aluminum alloy ruler.

### 3.6 Smoothing, Finishing, and Maintenance

After the first aluminum alloy ruler is scraped flat, use an iron trowel to smooth the traces of the aluminum alloy ruler on the concrete surface. After the second aluminum alloy ruler is scraped flat, use a polishing machine to polish it. When there is no trace of the iron trowel on the concrete surface, finish the concrete surface. The conventional water storage method is used for maintenance.
In Figure 2 and 3, the steel fiber distribution density is extremely high, which fully changes the brittleness of concrete, improves the toughness and ductility of the concrete slab, and increases the allowable bending deflection of the slab. The steel fiber is distributed in three dimensions in the concrete from the bottom of the floor. The concrete can be reinforced from all directions, and the density is extremely high. It can effectively improve the bonding and bite force between the steel fiber and the aggregate, improve the floor's resistance to cracking, improve the hollowing phenomenon, and effectively ensure the integrity of the floor.

**Figure 2**: Finishing the Surface

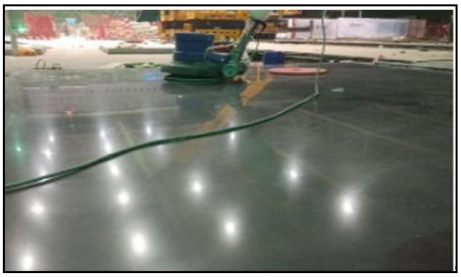

**Figure 3**: Grinding and Polishing

## 4 QUALITY CONTROL MEASURES

Before construction, be familiar with the construction drawings, prepare the construction plan according to the requirements of the design drawings and the current national standards and process regulations, and conduct technical briefings to the team to ensure that they understand the flatness requirements and construction methods, and carry out the construction of the sample section. Check the base to ensure that the base is flat, solid and crack-free.

According to the size of the concrete floor area and the span of the plant each time, the spacing of the adjustment bolts and angle steels should be reasonably set. The channel steel should be installed firmly and straight and flat, and the adjustment bolts and angle steels used should be installed firmly. The angle steel elevation should be within the error range and the elevation measurement should be accurate. It is strictly forbidden to collide with the adjustment bolts and angle steels during construction. If damage occurs, re-measure and install them in time. Use tools such as level, ruler, laser leveler, etc. for real-time detection and adjustment during the construction process. Control the mix ratio of concrete and mortar to ensure stable material performance.

When vibrating with a vibrator, the vibration time of each vibration point should be based on the presence of floating slurry on the concrete surface, no bubbles, and no longer settling. When using an aluminum alloy ruler to manually scrape and level, the force should be uniform and coordinated, and the concave parts should be filled and leveled in time. Repeated sawing and scraping, the parts where the angle steel is removed should be scraped and leveled in time, and local parts should be leveled with wooden or iron trowels. After the concrete is poured on the ground, it should be watered and maintained in time. The maintenance time should not be less than 7 days. When the temperature is below 5℃, insulation measures should be taken and watering maintenance should not be carried out [1]. Post-construction inspection should be carried out, and the flatness of the floor should be checked with a two-meter ruler. Parts that exceed the allowable error should be repaired.

## 5 SAFETY AND ENVIRONMENTAL PROTECTION MEASURES

During the installation of channel steel and angle steel, workers should cooperate with each other, and the process of hammering bolts and reinforcements should be highly focused to avoid workers being injured. After the channel steel, angle steel and other materials are brought into the site, they should be classified and placed neatly according to the requirements of the plane layout, and clearly marked. It is strictly forbidden for concrete transport vehicles to sound the horn when entering and leaving the site at night, and materials should be handled with care when loading and unloading. For construction machinery and tools that generate noise and vibration, noise reduction, sound absorption and sound insulation measures should be taken. After the construction of channel steel, angle steel and other materials is completed, the surface is cleaned uniformly, and then anti-rust measures are taken and reused.

## 6 CONCLUSION

With the development of the construction industry, the quality control of building and structural floor construction is becoming more and more important. In particular, the control of the flatness of large-volume concrete surfaces in actual construction is a big problem, which requires comprehensive consideration of materials, processes and quality control.

## COMPETING INTERESTS

The authors have no relevant financial or non-financial interests to disclose.

**REFERENCES**

[1] Nie Gengxiang. Construction quality control of large-area concrete wear-resistant floor engineering. Construction Technology Development, 2013(12):34-37.
[2] Xu Guoliang, Zhang Guangzhi, Wang Guolan. Exploration of new technology for controlling the elevation and flatness of large-area wear-resistant floor. Scientific Research, 2015(13):154.
[3] Gao Fangsheng, Yang Lin, You Lifeng, et al. New technology of skip-bin construction. Construction Technology, 2011, 42(5):431–435.
[4] Li Tiebing, Chen Xiyang, Wang Jun, et al. Construction of reinforced concrete structural slabs with high flatness requirements. Construction Technology, 2011, 42(9):823–826

**World Journal of Engineering Research**
**ISSN: 2959-9873**
**DOI: 10.61784/wjer3002**

# CRACK CONTROL TECHNOLOGY FOR THE OVERALL FLOOR OF AN ULTRA-LONG AND LARGE EXHIBITION HALL

WenHeng Sun[1,2], XiaoJu Zhang[1,2,*], XuanZhong Luo[1,2], ZhiCheng Bai[1,2], ZhiYuan Zhang[1,2]
*[1]China Construction Fourth Engineering Bureau Co., Ltd. Guangzhou, Guangdong 510000, China;*
*[2]China Construction Fourth Engineering Bureau Sixth Construction Co., Ltd. Hefei, Anhui 230000, China.*
*Corresponding author: XiaoJu Zhang, Email: 19822660870@163.com*

**Abstract:** Construction cracks are prone to occur in the construction of large-area flooring, which affects the integrity, aesthetics and quality of the flooring. How to better control construction cracks has become an important issue that construction units must consider. This article will analyze the specific causes and control techniques of construction cracks in large-area flooring of buildings based on actual conditions, in order to provide reference and reference for related construction operations.
**Keywords**: Large-area flooring; Cracks; Construction; Exhibition hall

## 1 INTRODUCTION

With the gradual acceleration of urbanization and modernization in my country, more and more large public buildings are under rapid construction, such as colleges and universities, airports, large stadiums, hospitals, large factories and other buildings. These buildings have a common feature, that is, the length of a single building is long, the area is large, and the construction period is tight. During the construction of the building, there will be super-long and large-area floors. Super-long and large-area floors will produce small cracks under the action of temperature shrinkage creep, which will cause quality hazards such as seepage and leakage in the later stage [1-4]. Therefore, how to effectively reduce the generation of super-long area concrete temperature cracks is a technical problem that every construction technician has to overcome. Diamond abrasive concrete wear-resistant floor has been widely used in commercial and office building projects due to its excellent wear resistance, excellent durability, high reliability and convenient maintenance.

## 2 PROJECT OVERVIEW

A certain exhibition project has a total of 8 steel structure exhibition halls, central corridors and supporting rooms. Due to its functional requirements, different exhibitions need to be arranged. The exhibition hall floor is required to withstand the impact of heavy loads and meet the durability requirements. The underground floor is a large-area concrete floor, which should be considered comprehensively.

## 3 DESIGN OF CRACK CONTROL TECHNOLOGY FOR LARGE-AREA FLOOR CONSTRUCTION

During the construction of large-area floor, cracks are prone to occur due to the constraint of concrete deformation. Therefore, in order to effectively control cracks, high-performance casting materials need to be configured. First, it is necessary to determine the configuration principle of casting materials. The casting materials on the upper and lower sides of the floor are different, and the constraint stress and friction coefficient are different. Therefore, asphalt can be appropriately added to the casting materials to compensate for shrinkage deformation. There is also a constraint between the casting materials and the columns. Therefore, partitions can be made in advance to determine the constraint strength of the front and rear poured concrete, reduce the constraint tensile stress, and add mortar to the casting materials to avoid evaporation of material water.
During the construction process, it is necessary to effectively control the hydration heat of concrete. Therefore, this paper selects the TSTM stress testing machine to quantitatively analyze different types of concrete mixtures, and selects the casting concrete that meets the construction requirements according to the obtained parameters.
This paper selects the TSTM stress testing machine to quantitatively analyze different types of concrete mixtures, and selects the pouring concrete that meets the construction requirements based on the obtained parameters. When pouring the floor in special foundations such as rock, a sliding layer is required to reduce the cushion constraint. Steel fiber and polypropylene fiber can effectively increase the tensile strength of the pouring material. Therefore, the technology designed in this paper uses orthogonal processing, and the parameters of different test blocks are shown in Table 1.
As can be seen from Table 1, by comparing the above test blocks, the trial strength $f_{cu}$ of the pouring material can be calculated

**Table 1** Parameters of Different Test Blocks

| serial number | A steel fiber content (%) | B Polypropylene content (%) | C Polypropylene aspect ratio |
|---|---|---|---|
| 1 | 1 | 1 | 1 |
| 2 | 1 | 2 | 2 |
| 3 | 1 | 3 | 3 |
| 4 | 2 | 1 | 2 |
| 5 | 2 | 2 | 3 |
| 6 | 2 | 3 | 1 |
| 7 | 3 | 1 | 3 |
| 8 | 3 | 2 | 1 |
| 9 | 3 | 3 | 2 |
| 10 | 0 | 0 | - |

$f=f_{cuk}+\sigma$ （1）

Wherein, fcuk represents the trial strength, and σ represents the standard deviation of lightweight aggregate. According to the above-mentioned matching strength of the casting material, the amount of cement can be determined and the density grade of the lightweight aggregate can be adjusted. In order to meet the high-strength goal of floor construction, this paper uses the slump interpolation method to adjust the amount of clean water and determine the volume sand ratio. At this time, the total volume VS of coarse and fine aggregates can be calculated according to the bulk density relationship of the material:

$V_S=V_T\times S_p$ （2）

Wherein, VT represents the volume of fine aggregate, and SP represents the volume sand ratio. Combined with the above-mentioned floor casting material preparation parameters, high-performance floor casting materials can be mixed to reduce the risk of cracks in floor construction.

## 4 LIGHTWEIGHT HEAVY-LOAD FLOOR DIAMOND SURFACE CRACK CONTROL

### 4.1 Problems with Diamond Wear-Resistant Floor

Just like Figure 1, diamond floor is mainly composed of high-strength cement, inorganic wear-resistant aggregate and pigment powder. In the initial stage of construction, the surface is treated with corresponding technical methods to achieve a solid, durable and beautiful effect. Because this type of floor has good impact resistance and compression resistance, it is widely used in industrial sites, docks, parking lots, logistics warehouses and other buildings. However, the construction technology of diamond abrasive floor is strict. Some construction units carry out on-site construction without correctly grasping the application points, resulting in many quality defects in the floor. It is easy to have disease problems in subsequent use, and cracks are one of the most common problems. The emergence of quality problems makes it lose its flatness, which not only affects its use, but also causes certain hidden dangers.

**Figure 1** Cracks in Corundum Floor

### 4.2 Methods for Repairing Cracks in Corundum Wear-Resistant Floor

(1) Repair with pure corundum. Repair with pure corundum can effectively solve the color difference problem, make the crack repair position consistent with the color of the overall floor, and have good aesthetics. In the application of the pure corundum repair method, it should be noted that the corundum aggregate used needs to be filled in two times to ensure that the filling is dense and full. The pure corundum repair method also has certain disadvantages. During the repair process, the corundum and concrete are not firmly bonded, and it is easy to fall off, and the durability is poor.

(2) Repair with corundum mixed with cement. The repair method of corundum mixed with cement can make the contact between the filler and the floor more firm, and achieve higher strength and good durability. However, since the cement material used will appear white after solidification, it has a significant color difference from the original corundum floor, and the overall aesthetics is poor. From the perspective of use, this method has great limitations.

(3) Repair with corundum mixed with yellow sand and resin. The repair method of diamond sand mixed with yellow sand and resin has the advantages of high strength, no obvious color difference, good durability, etc. However, before the repair begins, the crack position must be cleaned in detail to ensure that there are no impurities before repairing. The repair work must be poured in batches, and the grinder can be used for polishing one week after the repair is completed.

## 5 CONCLUSION

The crack problem should not be underestimated. We should pay attention to it, study it more and improve it. It can bring the quality of the project to a higher level, and safety, quality and production can all be improved.

## COMPETING INTERESTS

The authors have no relevant financial or non-financial interests to disclose.

## REFERENCES:

[1] Gan Haitao. Crack control technology for large-area floor construction. China Building Metal Structure, 2023(09):35-37.
[2] Li Zuquan. Study on the influence of concrete mix ratio on the crack resistance of bridges and its mechanism. Civil Engineering, 2024(06):29-31.
[3] Zheng Yongsheng. Application of skipping method in the construction of 300 m long and large-volume concrete basements. Construction Technology Development Engineering Technology, 2022(11):112-115.
[4] Zhang Yongfu. Crack control of diamond wear-resistant floor. Sichuan Construction, 2023(09):106-108.

**World Journal of Engineering Research**
**ISSN: 2959-9865**
**DOI: 10.61784/wjer3003**

# INTEGRATED APPLICATION OF CADMIUM TELLURIDE THIN-FILM MODULES IN CURTAIN WALL ROOFS

XiaoJu Zhang[1,2], YinGuang Wang[1,2*], ShenShen Zhu[1,2], XiaoXia Zhao[1,2], YueQiang Cao[1,2], ZhiCheng Bai[1,2]
[1]*China Construction Fourth Engineering Bureau Co., Ltd. Guangzhou 510000, Guangdong, China.*
[2]*China Construction Fourth Engineering Bureau Sixth Construction Co., Ltd. Hefei 230000, Anhui, China.*
*Corresponding Author: YinGuang Wang, Email: 2557841138@qq.com*

**Abstract**: As an important place for display and communication, the design of large exhibition halls must not only meet the requirements of aesthetics and functionality, but also be combined with its subsequent use and green construction. This paper aims to deepen the photovoltaic design of the skylight of large exhibition halls, considering its large area, ground-based structure and lighting projection area, and explore how to make full use of renewable energy such as light energy and heat energy while ensuring aesthetics and functionality. A set of perfect design and construction methods are proposed, and verified and applied through actual cases.
**Keywords:** Cadmium telluride film; Large exhibition hall; Curtain wall design; Curtain wall roof; Key technology; Application case

## INTRODUCTION

With the increasing global climate change, it is particularly important to promote green planning, green design, green investment, green construction, green production, green circulation, green life and green consumption in an all-round and full-process manner. In the context of the intensification of global climate change and the depletion of renewable energy, how to make development and construction based on the efficient use of resources, strict protection of the ecological environment and effective control of greenhouse gas emissions, and how to use technical means to promote green construction and green construction to a new level. To achieve the above goals, we explore the potential of building construction under the premise of always adhering to the primary premise of green construction, and through architectural design methods, we start from the effective use of energy, while ensuring its architectural aesthetics and functionality, and maximize the use of clean, safe, inexhaustible and inexhaustible energy. Ensure the implementation of green buildings to ensure the realization of carbon peak and carbon neutrality goals, and promote my country's green development to a new level [1].
This paper aims to deepen the design and use of skylights in large exhibition halls, deepen the photovoltaic design of skylights, and explore how to make full use of light energy and heat energy while ensuring aesthetics and functionality requirements, so as to increase the proportion of green energy and renewable energy [2]. According to the large-scale and ground-type design characteristics of the exhibition hall, through the analysis and research of photovoltaic materials, structural design, construction technology and other aspects, a set of perfect design and construction methods is proposed to provide reference and guidance for the integrated design of renewable energy and curtain wall structure of large exhibition halls. At the same time, it will further advance the development of photovoltaic building integration [3].

## 1 PROJECT OVERVIEW

The first phase of the Hangzhou Convention and Exhibition Center is a large-scale comprehensive exhibition hall project, mainly composed of standard exhibition halls, conference centers, grandstand exhibition halls, and central corridor service spaces; the total construction area of the project is 1.22 million square meters, of which the first phase project has a total of 8 exhibition halls and central corridors, with a construction area of 64.32 square meters, an area of 215,700 square meters, a single-story above ground (partial double-story), a top design elevation of 42.36 meters, a curtain wall horizontal span of about 184 meters, a cornice aluminum plate system of 12,000 square meters, a cantilever structure height of 25.8 meters to 42.36 meters, a cantilever arc of 18 to 40 degrees, and a photovoltaic curtain wall area of 7841 square meters. The total installed capacity of photovoltaic power generation is 771.88kWp, with 3,356 pieces of 30% light-transmitting cadmium telluride thin-film photovoltaic glass and about 326 pieces of special-shaped non-power-generating glass installed. After the completion of the project, the annual power generation is expected to reach 700,000 kWh, which will become the "Linkong cover, Hangzhou showcase, and a new highland for national exhibition business". Large-scale exhibition halls are the main supporting carriers for urban display and communication. Their green energy use and system are important components of the curtain wall system. Their performance and structure requirements are higher, and various structural parameters need to be considered comprehensively during the design process.

## 2 KEY TECHNOLOGY SELECTION AND INTEGRATION

Under the dual carbon goals, renewable energy is used in a variety of ways. In order to promote the sustainable use of

renewable energy, the implementation of photovoltaic facilities has been accelerated. In order to achieve the dual carbon goals as soon as possible, green energy building integrated facilities have emerged. In view of the large-scale exhibition hall projects with large land occupation and ground-type design characteristics, the photovoltaic building integrated engineering exhibition continues to move forward, and it is particularly important to select high-efficiency and high-utilization regeneration systems.

### 2.1 Traditional Monocrystalline Silicon Solar Cell System

Currently, crystalline silicon materials (including polycrystalline silicon and monocrystalline silicon) are the main photovoltaic materials, with a market share of more than 90%, and will continue to be the mainstream material for solar cells for a considerable period of time in the future.

Using high-purity monocrystalline silicon rods as raw materials, monocrystalline solar cells have high photoelectric conversion efficiency (conversion rate is between 15.4%-26.3%), and stand out in photovoltaic applications.

The monocrystalline silicon solar cell panel is fixed on an aluminum plate with a copper tube on the back to form a system. The team compared the photovoltaic thermal system with the photovoltaic solar thermal deposition system. The analysis results show that the overall energy efficiency of the photovoltaic thermal system is close to the solar thermal deposition system, and photovoltaic thermal has a higher firefighting efficiency than the other two systems. In order to simulate the various parameters of the calculation system, the simulation results show that the electrical performance, thermal efficiency, total conversion efficiency and thermal utilization efficiency of the system are 10.01%, 17.18%, 45.00% and 10.75% respectively.

### 2.2 Polycrystalline Silicon Solar Cell System

Polycrystalline silicon solar panels are usually made of discarded monocrystalline silicon tailings or metallurgical silicon materials, and their cost is lower than that of monocrystalline silicon. Monocrystalline silicon solar panels are developed on the basis of solar panels, of which the photovoltaic industry accounts for 70%. The photoelectric conversion efficiency of polycrystalline silicon solar cells is usually lower than that of photovoltaics. The conversion efficiency of monocrystalline silicon solar panels with the highest speed is about 20.89%. The temperature coefficient of crystalline silicon solar cells is relatively high; the photoelectric conversion efficiency of crystalline silicon solar cells decreases more significantly with the increase of their own temperature; how to effectively use the heat absorption layer to remove the heat of crystalline silicon solar panels in time; the production cost of crystalline silicon solar cells is high, and their low-light performance is poor. Therefore, the performance of crystalline silicon solar cells needs to be further improved.

### 2.3 Cadmium Telluride Thin Film Curtain Wall System

Compared with other solar cells, the structure of cadmium telluride thin film solar cells is relatively simple, usually composed of five layers, namely glass substrate, transparent conductive oxide layer, cadmium sulfide (CdS) window layer, cadmium telluride absorption layer, back contact layer and back electrode.

Cadmium telluride is a direct gap semiconductor, its gap width is very well matched with the solar spectrum, and its gap width can work normally at high ambient temperature, with good radiation resistance. In addition, cadmium telluride solar cells are composed of polycrystalline thin films, and the preparation process is relatively simple. Therefore, the application of cadmium telluride solar cells is very promising, especially for high-altitude and desert power plants, outer space and deep space energy, and as compressed batteries. Electrical performance parameters can be seen in Table 1, and Mechanical parameters can be seen in Table 2.

**Table 1** Electrical Performance Parameters

| model | JC-RTN | | | |
|---|---|---|---|---|
| Pattern form | Royal blue | Royal blue | Yellow | Green |
| Power | 65Wp | 85Wp | 85Wp | 85Wp |
| Power tolerance | ±5 | | | |
| Short circuit current | 0.71A | 1.13A | 1.08A | 1.06A |
| Open circuit voltage | 117.2V | 118.4V | 118V | 117.2V |
| Peak power current | 0.52A | 0.97A | 0.91A | 0.92A |
| Peak power voltage | 72V | 97.1V | 94.7V | 90.1V |

**Table 2** Mechanical Parameters

| | | | |
|---|---|---|---|
| Component dimensions | 1200×600×9.34mm | Battery type | Cadmium telluride thin film |
| Weight | 16.8kg | area | 0.72m$^2$ |
| Connection box | Back or side connection, cable2.5mm$^2$，650±10mm | | |
| Connector | MC4 or MC4 compatible | | |
| Structure | 3.2mmCdTe+0.38mmPVB+0.76mmPVB+5mm | | |

## 3 INTEGRATED APPLICATION OF CADMIUM TELLURIDE CURTAIN WALL AND ROOF IN LARGE EXHIBITION HALLS

### 3.1 Key Scientific and Technological Points Taking the Photovoltaic Roof of Hangzhou Convention and Exhibition Center as an Example

In the construction of the photovoltaic curtain wall project of the skylight roof, cadmium telluride thin film modules were applied to the construction of the integrated photovoltaic project of the building for the first time. Under the premise of ensuring the primary requirements of the structural transmittance, cadmium telluride light-transmitting modules with a transmittance of 30% were used to generate more than 700,000 kWh of electricity per year, which is equivalent to the lighting power consumption of the basement and ground offices of Hangzhou Convention and Exhibition Center, and equivalent to planting more than 30,000 trees next to the building.

In the photovoltaic integration construction, cadmium telluride photovoltaic modules with a single capacity of 320Wp were used, and 3,356 single 320Wp modules were installed. The total photovoltaic capacity is 771.88kWp. The photovoltaic module layout adopts the roof flat laying method, with 6/7 photovoltaic modules as a group, and 3 groups are equipped with a set of photovoltaic return kits, and 1*6mm$^2$ photovoltaic lines are used to lead to the inverter in the distribution room through the cable trough box. The project is equipped with 10 inverters, and every 5 inverters are connected to a low-voltage cabinet grid-connected cabinet. This project uses 2 400V low-voltage grid-connected cabinets, and uses 2 transformers for power consumption. The power generation form is self-generated and self-used, and the surplus power is connected to the grid. While meeting the light transmission requirements of the skylight, combined with power generation, the subsequent use efficiency is improved, and the use of green energy for environmental protection is promoted. At the same time, the use of assembly components saves a lot of maintenance costs compared with traditional processes, reduces material waste and environmental pollution, and is in line with the development trend of green and low-carbon buildings in my country.

### 3.2 Main Construction and Installation Technical Measures

The construction method of cadmium telluride thin-film photovoltaic roof installation mainly includes nine parts: measurement and re-measurement and photovoltaic component installation, system debugging, array line construction, junction box installation, photovoltaic inverter installation, distribution panel cabinet installation, cable laying, lightning protection and grounding construction, and trial operation.

#### *3.2.1 Measurement and component installation*

1. Construction measurement and layout

The basis for construction measurement includes plan layout drawings, construction drawings, and positioning control points of the construction site. The main contents of construction measurement include checking coordinate points, laying out points based on coordinate points, and related openings.

2. Photovoltaic bracket and component installation plan

The photovoltaic components are fixed to the original roof frame with bolts; the flatness of the original roof frame and the deflection of the supporting beam are re-measured; if it exceeds the specified range, the corresponding construction party needs to make rectifications; re-measure the reserved holes, and compare the position of the pressing block and the size of the components and small frames to see if they meet the installation requirements.

4) Photovoltaic component installation

During transportation and storage, the components should be handled with care, without strong impact and vibration, and should not be placed horizontally and heavily. Prevent hidden cracks in the battery and affect operating efficiency. The components should be installed from bottom to top, one by one, and must be handled with care during the installation process to avoid damaging the surface of the components. The components must be installed horizontally and vertically, and the spacing between the components in the same square array should be consistent; pay attention to the direction of the component's junction box. The connection between the components and the bracket system can be installed using the mounting holes on the frame, clamps or embedded systems. Just like Figure 1-4, the installation of components must be carried out in accordance with the following examples and suggestions.

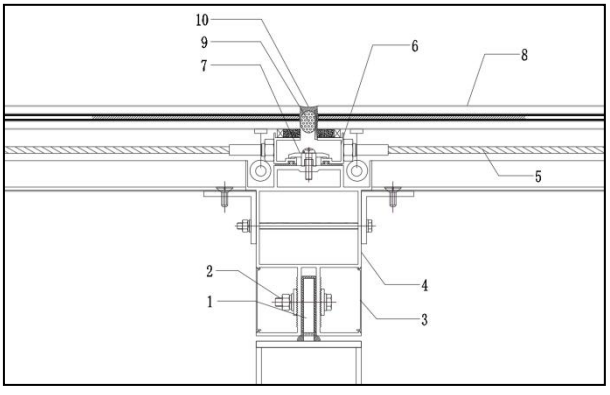

**Figure 1** Schematic Diagram of Photovoltaic Module Installation

1-Steel plate; 2-Stainless steel bolts; 3-Aluminum alloy buckle cover; 4-Aluminum alloy main keel; 5-Stainless steel anti-fall rope; 6-Aluminum alloy auxiliary frame; 7-Aluminum alloy block; 8-High-transmittance photovoltaic glass (8mm ultra-white tempered glass + 1.52mmPVB + 3.2mm cadmium telluride power generation glass + 1.52mmPVB + 8mm ultra-white tempered glass); 9-Aluminum alloy support strip; 10-Silicone sealant.

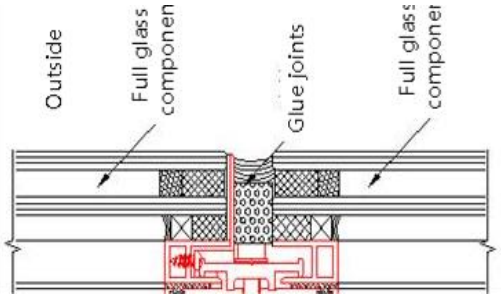


**Figure 2** Schematic Diagram of Photovoltaic Module Installation

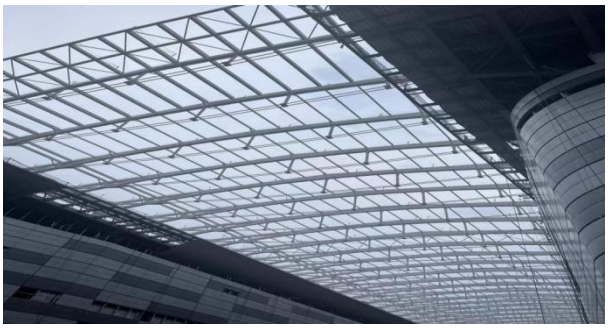

**Figure 3** Roof Truss Span Structure Diagram

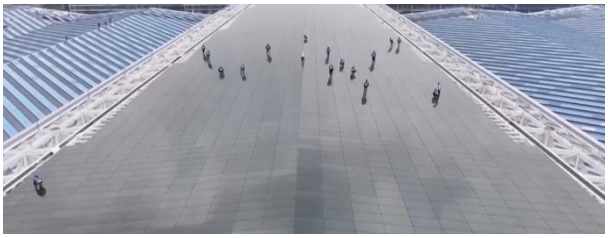

**Figure 4** Photovoltaic Roof Installation Effect Diagram

## 4 PHOTOVOLTAIC CURTAIN WALL ROOF QUALITY CONTROL

The use of this process is closely related to the quality control during the use of the process. During the construction and use, attention should be paid to the process quality and comprehensive quality problems should be dealt with.

A quality reward and punishment system should be established. According to the implementation of the system, everyone should clarify their respective quality responsibilities. Organize construction personnel to study the "Specifications", "Verification Standards", relevant technical documents and materials of the manufacturer, instructions and design requirements of the design institute, so that construction personnel can clarify the quality standards, master the installation and commissioning processes, and ensure the installation quality.

Before the project construction, the engineering quantity should be counted first, and the progress of the project should be arranged reasonably. Construction personnel must strictly carry out construction according to the construction organization design and the contents of quality, technology and safety disclosure, and do a good job of recording various original data.

When the bolt connection parts and bolt hole positions are inconsistent, fire welding shall not be used for cutting, and only re-drilling and adjustment can be made. Welding materials should be selected according to relevant regulations, and the welding materials used should have a supplier's warranty.

When handling equipment defects, we should take the initiative to work with the technical personnel and supervisors of the relevant parties to study and formulate solutions suitable for on-site construction. Carefully inspect and record all kinds of equipment defects and unqualified products, and handle them according to the requirements of the specifications.

## 5 CONCLUSION AND PROSPECT

Through the research on the integrated application of cadmium telluride thin film modules in curtain wall roofs based on the first phase of the Hangzhou Conference Center project in Hangzhou, the following conclusions can be drawn: With the improvement of building energy-saving requirements, new building energy-saving materials are also developing continuously. In order to significantly reduce the energy consumption of buildings, traditional photovoltaic roofing materials are mostly metal roofing + photovoltaic panel structures, which can no longer meet the requirements of large exhibition halls for energy saving, light transmission and beauty. The new technology of building and energy-saving integration has become an important direction for the development of green and low-carbon building energy-saving systems, and the technological development from energy saving to green power generation has become the next journey that the construction industry needs to move forward. Reasonable analysis of the application of each node, comprehensive economic considerations, and implementation after expert demonstration, the construction process is efficient and reliable, and possible problems are anticipated in advance and solved through technical means, saving construction costs and accelerating construction progress. At the same time, it creates favorable conditions for the integrated construction of photovoltaic buildings and has broad application prospects.

In order to implement the new technology of building and energy-saving integration, the following three technical difficulties need to be solved: first, to ensure the original light transmittance requirements of the skylight; second, to ensure the overall quality and durability of the curtain wall roof; third, to improve the green energy flow of large exhibition halls and promote the low-carbon development of green buildings.

## COMPETING INTERESTS

The authors have no relevant financial or non-financial interests to disclose.

## REFERENCES

[1] China Academy of Building Research, Shanghai Academy of Building Research (Group) Co., Ltd. Green Building Evaluation Standard GB/T50378-2014 Table 5.2.16 Renewable Energy Utilization Scoring Rules. Beijing: China Building Industry Press, 2015.

[2] Nietic S, Cabo F G, Kragic I M, et al. Experimental and numerical investigation of a backside convective cooling mechanism on photovoltaic panels. Energy, 2016, 111: 211-225.

[3] Chen Hongbing, Niu Haoyu, Zhang Lei. Experimental study of heat pipe solar PV/T heat pump system under heating and collection mode. Renewable Energy, 2017, 35 (12): 1791-1797.

**World Journal of Engineering Research**
**ISSN: 2959-9873**
**DOI: https://doi.org/10.61784/wjer3004**

# RESEARCH ON MICRO-DISTURBANCE PRE-CONTROL TECHNOLOGY FOR SUBWAY SIDE FOUNDATION PIT

XiaoXia Zhao[1,2], ZhiCheng Bai[1,2*], Tao Kong[1,2], MinJian Long[1,2], Bing Yang[1,2]
[1]*China Construction Fourth Engineering Bureau Co., Ltd. Guangzhou 510000, Guangdong, China.*
[2]*China Construction Fourth Engineering Bureau Sixth Construction Co., Ltd. Hefei 230000, Anhui, China.*
*Corresponding Author: ZhiCheng Bai, Email: 19822660870@163.com*

**Abstract:** With the continuous deepening of the development and utilization of urban underground space, how to carry out deep foundation pit construction next to the subway while ensuring the safety of subway operation has become a major challenge in the engineering field. Taking the Hangzhou Convention and Exhibition Center project as an example, this study explores the safety control of long and deep foundation pit construction next to the subway through micro-disturbance pre-control technology under high-density rail transit environment. This paper first analyzes the geological conditions and construction environment of the project, then constructs an empirical prediction function that affects tunnel deformation, and proposes the foundation pit support control concept of "early isolation, strong block division, soft pit division". Based on three-dimensional finite element analysis, the effectiveness of the proposed technology is verified, providing a theoretical basis and practical guidance for similar projects.
**Keywords:** Subway side foundation pit; Micro-disturbance pre-control technology; Deformation control; Finite element analysis; Hangzhou convention and exhibition center

## INTRODUCTION

The "14th Five-Year Plan" released by the state in 2021 proposes to build a "resilient city" and improve the city's ability to cope with risks. The efficient and reasonable development and utilization of underground space is an important part of the construction of a "resilient city". Therefore, in the next few years, the scale of underground space development and utilization will be further expanded, and it will show a larger, deeper and more three-dimensional development trend. In the process of underground space development and utilization, the high-density distribution of urban rail transit has led to the emergence of a large number of deep foundation pit projects close to the subway. The subway shield tunnel is extremely sensitive to changes in the surrounding environment. Improper construction may affect the structural safety and normal operation of subway facilities.

## 1 PROJECT OVERVIEW

The Hangzhou Convention and Exhibition Center project is located in Nanyang Street, Xiaoshan. There are scattered residential houses and industrial plants on the northwest side of the site, and the operating Metro Line 1 is under the middle of the site. The roads around the project include the Meishi Line, Nanfeng Line, Yannan Line, Gangcheng Avenue (main road) and the planned Zhemei Road Tunnel, with convenient transportation. The underground building area is 220,000 square meters. The project is divided into foundation pits on both sides of the north and south areas, with the shield tunnel of Metro Line 1 in operation (crossing from east to west). The minimum distance between the two foundation pits is 40.8 meters, and there is a connecting passage above the tunnel.

## 2 RESEARCH ON PRE-CONTROL INDICATORS OF LONG AND DEEP FOUNDATION PITS BESIDE OPERATING SUBWAYS

In terms of deformation control of existing tunnels, relevant specifications have been proposed one after another, such as: "Technical Specifications for Safety Protection of Urban Rail Transit Structures" (GJJ/T202-2013) proposed a warning value of 10mm and a control value of 20mm for horizontal and vertical displacements of tunnels; on the basis of national standards, Zhejiang Province's "Technical Regulations for Safety Protection of Urban Rail Transit Structures" (DB33/T1139-2017) divides the control indicators of horizontal and vertical displacements of shield tunnels into four levels, namely horizontal displacement: 5mm, 8mm, 14mm, 20mm; vertical displacement: 5mm, 10mm, 15mm, 20mm. Strict deformation control standards put forward higher technical requirements for the prediction of tunnel deformation before construction and the setting of corresponding protection measures. Cases of Excavation Projects beside Existing Tunnels can be seen in Table 1.

**Table 1** Cases of Excavation Projects beside Existing Tunnels

| No. | Project name | Adjacent to subway | Tunnel top burial depth $h$（m） | Pit depth $H$（m） | Pit length $L$（m） | Horizontal spacing $l$（m） | Tunnel maximum deformation $S$ | | Soil reinforcement measures in passive zone | Pit support |
|---|---|---|---|---|---|---|---|---|---|---|
| | | | | | | | Vertical deformation $S_v$（mm） | Horizontal deformation $S_h$（mm） | | |
| 1 | A foundation pit in Shanghai[1] | Line 4 | 15 | 13 | 75 | 5.5 | 6.5 | 11 | Three-axis cement mixing pile | Ground-anchored wall; row of piles |
| 2 | A deep foundation pit in Yangpu District, Shanghai[2] | Line 2 | 15.4 | 7.5 | 49 | 17 | 3.5 | 2 | Three-axis cement mixing pile | - |
| 3 | A foundation pit in Shanghai[3] | A station | 8.5 | 5.3 | 100 | 5.2 | 5.6 | 5.8 | Jet grouting reinforcement | Ground-anchored wall; bored piles; SMW pile isolation piles |
| 4 | A deep foundation pit in Shanghai World Expo Green Valley[4] | Cross-river tunnel | 16.3 | 9.6 | 200 | 6.7 | 5.6 | 6.1 | - | Ground-anchored wall |
| 5 | New Jiahe Wanggang Station[5] | Existing Jiahe Wanggang Station | 12 | 8.2 | 15 | 3.9 | 11 | 6.3 | - | Ground-anchored wall |
| 6 | Shanghai Daning Commercial Center[6] | Line 1 | 15.9 | 8 | 30 | 7.9 | 4.9 | 6.5 | Cement mixing pile | Gravity wall + row of piles |
| 7 | A foundation pit[7] | Line 1 | 13.4 | 6.4 | 100 | 3 | 8 | 11 | Three-axis cement mixing pile | Ground-anchored wall; bored piles |
| 8 | A foundation pit in Nanjing Road, Shanghai[8] | Line 2 | 11 | 10 | 100 | 3.2 | 5.4 | 5.9 | Jet grouting pile reinforcement | Ground-anchored wall |
| 9 | A foundation pit in Shanghai[9] | Line 1 | 19.5 | 13 | 50 | 6.5 | 2.6 | 4 | Mixed pile skirt reinforcement | Ground-anchored wall |
| 10 | Jing'an Temple Station on Line 7[10] | Line 2 | 12 | 15.5 | 107 | 10 | 0.5 | - | Jet grouting pile reinforcement | SMW piles; jet grouting piles |
| 11 | Plot 1788, Nanjing West Road[11] | Line 2 | 16.9 | 11.4 | 114 | 9.5 | 6.5 | 7.1 | Three-axis cement mixing pile | Ground-anchored wall |
| 12 | Shanghai Huidefeng foundation pit[12] | Line 2 | 12.5 | 12.5 | 80 | 9 | 12 | 11 | Cement mixing pile skirt full-height reinforcement | Ground-anchored wall; SMW piles |
| 13 | A foundation pit in Shanghai[13] | Line 1 | 7 | 10 | 42 | 15 | 1.5 | 6.3 | Cement mixing pile full-height reinforcement | Ground-anchored wall |
| 14 | A | Line 2 | 10 | 16 | 130 | 17 | 3.3 | 5.9 | - | Ground-anchor |

| | | | | | | | | | | |
|---|---|---|---|---|---|---|---|---|---|---|
| | foundation pit in Hongqiao District, Shanghai[14] | | | | | | | | | ed wall |
| 15 | A foundation pit in Shanghai Plaza[15] | - | 10.8 | 6 | 100 | 4.8 | 4.8 | 4.6 | High-pressure jet grouting pile | Ground-anchored wall; bored piles |
| 16 | A foundation pit in Pudong District, Shanghai[16] | Line 4 | 8.7 | 19.5 | 87 | 3 | 3 | 5.5 | - | Ground-anchored wall |
| 17 | A foundation pit in Huaihai Middle Road, Shanghai[17] | Line 1 | 29.1 | 24.3 | 211 | 5 | 12 | 9.5 | SMW method pile full-height, strip drawing | Ground-anchored wall |
| 18 | A foundation pit in Suzhou[18] | Line 3 | 22.5 | 14 | 100 | 8.5 | 17 | 14 | - | Ground-anchored wall; bored piles |
| 19 | A foundation pit in Suzhou[19] | Line 4 | 12.5 | 12.5 | 80 | 9 | 1.51 | 6.32 | - | Ground-anchored wall |
| 20 | A foundation pit in Hangzhou[20] | - | 15.4 | 7.5 | 49 | 17 | - | 2 | Skirt strip drawing reinforcement; Mixed pile | Ground-anchored wall; bored piles |
| 21 | A foundation pit in Tianjin[21] | - | 15 | 15 | 75 | 16.5 | 7.4 | 13 | - | Ground-anchored wall; isolation piles; bored piles |
| 22 | A complex building in Guangzhou[22] | - | 5 | 18 | 92 | 15 | 4 | 5 | - | Ground-anchored wall |
| 23 | A foundation pit in Ningbo[23] | Line 1 | 12 | 11.4 | 120 | 16.4 | 5.3 | 7.5 | Cement mixing pile | Drilled piles; retaining piles |

Just as Figure 1-4 and Table 2, for the side foundation pit, the main factors affecting the cumulative deformation S of the tunnel include: tunnel top burial depth h, foundation pit depth H, foundation pit length L, and horizontal distance l between the foundation pit and the tunnel.

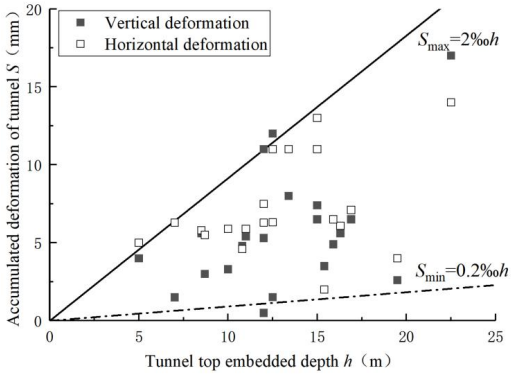


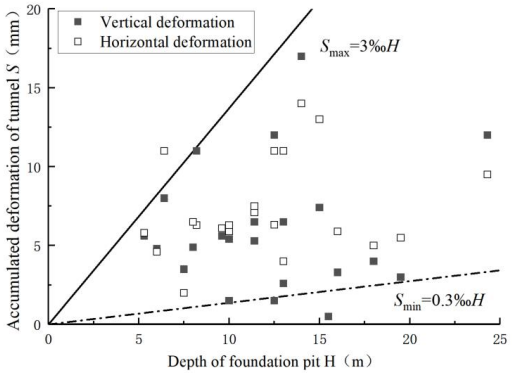

**Figure 1** Relationship between Tunnel Cumulative Deformation and Tunnel Top Burial Depth *h*

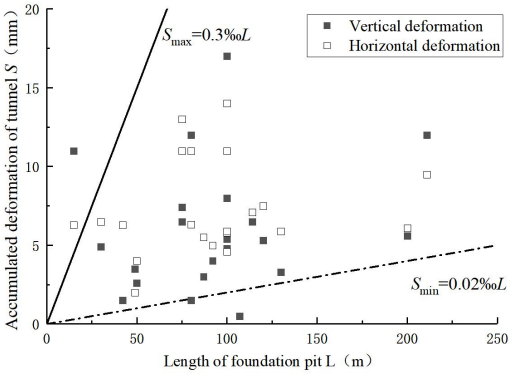


**Figure 2** Relationship between Tunnel Cumulative Deformation and Foundation Pit Excavation Depth *H*

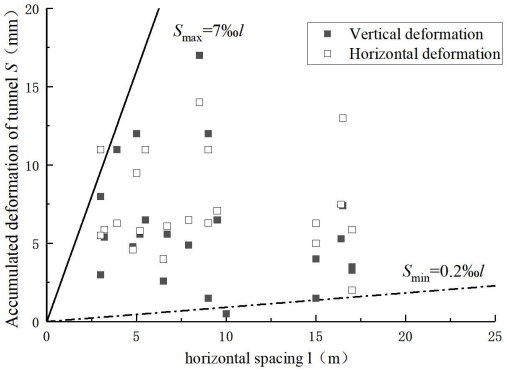


**Figure 3** Relationship between Tunnel Cumulative Deformation and Foundation Pit Length *L*

**Figure 4** Relationship between Tunnel Cumulative Deformation and Horizontal Spacing *l*

**Table 2** Statistics of the Impact of Side Foundation Pits on Tunnel Structure

| Proportional coefficient | Range of variation | Mean |
|---|---|---|
| ($S/h$) | 0.2‰-2‰ | 1.1‰ |
| ($S/H$) | 0.3‰-3‰ | 1.65‰ |
| ($S/L$) | 0.02‰-0.3‰ | 0.16‰ |
| ($S/l$) | 0.2‰-7‰ | 3.6‰ |

Note: The order of magnitude of the foundation pit length *L* is 10 times that of the tunnel top burial depth *h*, foundation pit depth *H*, and horizontal spacing *l*. The order of magnitude of the four variables needs to be unified when comparing, that is, the average influence of the foundation pit length *L* is 1.6‰.

For the side foundation pit, the main factors affecting the cumulative deformation S of the tunnel structure are: tunnel top burial depth h, foundation pit depth H, foundation pit length L, and horizontal spacing l. The influence on the deformation of existing tunnels is from large to small in the order of horizontal spacing l> foundation pit depth H> foundation pit length L> tunnel top burial depth h.

Combining the above four influencing factors and a large number of existing tunnel side foundation pit engineering cases under sandy soil conditions, an empirical prediction function between the tunnel cumulative deformation Smax and the factor variables is established on this basis, assuming that g1 is a variable related to the foundation pit excavation form, and g2 is a variable related to the foundation pit construction protection measures.

$$S_{max}=g_1 h(l+\lg L)/H+g_2 \quad (1)$$

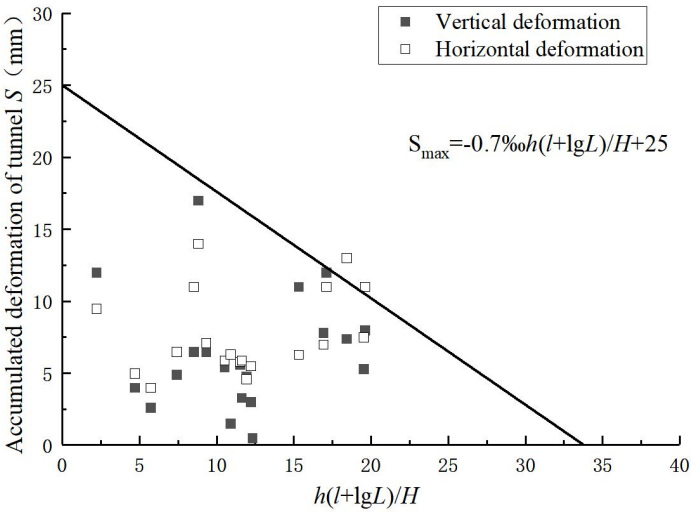


**Figure 5** Tunnel Cumulative Deformation Empirical Prediction Function

As shown in Figure 5, the empirical prediction function is obtained: $S_{max}$=-0.7‰$h(l+\lg L)/H$+25. Among them, $g_1$ is the function slope, indicating the speed of tunnel cumulative deformation, $g_1$=-0.7‰; $g_2$ is the function intercept, indicating the degree of influence, $g_2$=25mm.

In Table 3, taking the sandy soil area as the background, the tunnel cumulative deformation is uniformly divided into four levels: 5mm, 10mm, 15mm and 20mm, and the corresponding side foundation pit related parameters are predicted

respectively, as shown in the Table 3:

Table 3 Reference for Relative Position Indicators of Side Foundation Pit

| Tunnel top burial depth *h* (m); foundation pit depth *H* (m); horizontal spacing *l* (m); foundation pit length *L* (m) | | | | |
|---|---|---|---|---|
| Tunnel-pit vertical relative position *h*/*H* | Tunnel deformation limit 5mm | Tunnel deformation limit 10mm | Tunnel deformation limit 15mm | Tunnel deformation limit 20mm |
| ≤0.5 | *l*≥55m<br>*L*≤50m | *l*≥40m<br>*L*≤60m | *l*≥30m<br>*L*≤80m | *l*≥15m<br>*L*≤80m |
| ≤1 | *l*≥30m<br>*L*≤40m | *l*≥20m<br>*L*≤60m | *l*≥15m<br>*L*≤60m | *l*≥10m<br>*L*≤60m |
| ≤2 | *l*≥15m<br>*L*≤30m | *l*≥10m<br>*L*≤40m | *l*≥5m<br>*L*≤50m | *l*≥3m<br>*L*≤50m |
| ≤3 | *l*≥8m<br>*L*≤20m | *l*≥6m<br>*L*≤20m | *l*≥5m<br>*L*≤20m | *l*≥2m<br>*L*≤20m |

Based on the empirical conclusion of the relative position pre-control index of the side foundation pit, when the tunnel deformation limit is 15mm, the vertical relative position of the tunnel-pit h/H≤2, and the horizontal clear distance l≥5m. Combined with the calculation of the foundation pit working conditions, that is, the tunnel top burial depth h=11m, the foundation pit depth H=5.5m, the horizontal spacing l=6.5m, 11.7m, combined with the deformation experience prediction function (Smax=-0.7‰h(l+lgL)/H+25), it is recommended that the single foundation pit excavation length be controlled within 50m.

## 3 CONTROL CONCEPT OF LONG AND DEEP FOUNDATION PIT SUPPORT ON THE SIDE OF THE GROUND PROTECTION AREA

As shown in Figure 6 and 7, the construction control measures of the side foundation pit mainly include soil reinforcement in the passive area of the pit, foundation pit support structure and foundation pit excavation method. In the sandy soil area, the soil reinforcement is mainly cement soil mixing piles, and the plane layout of soil reinforcement includes full-chamber type, skirt type, and strip type. The vertical layout of passive zone soil reinforcement includes reinforcement below the pit bottom, and reinforcement below and above the pit bottom at the same time. Commonly used foundation pit support structures include ground-connected walls, bored piles, SMW piles, cement mixing piles, etc., and the impact of foundation pit construction on the surrounding environment is reduced by appropriately applying isolation piles. In addition, most excavation methods adopt layered and segmented excavation, and support while excavating.

(a) Full-Height Type (b) Skirt Type (c) Strip Type

**Figure 6** Plane Layout of Soil Reinforcement in the Passive Area of q

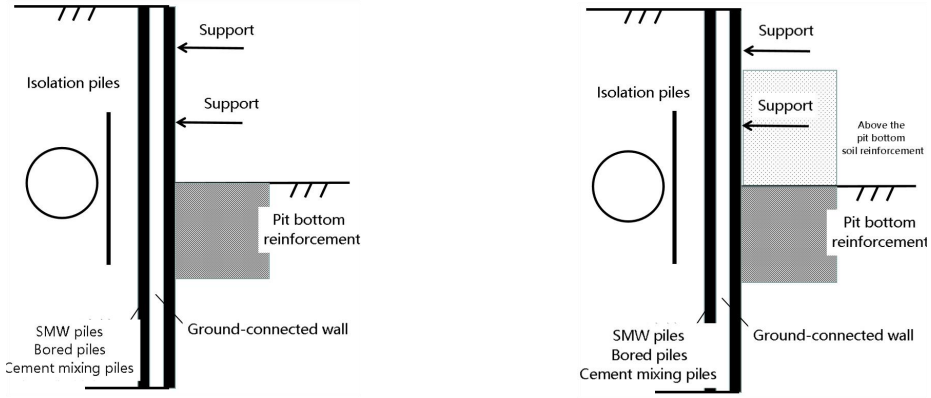


(a) Reinforcement below the Pit Bottom

(b) Simultaneous Reinforcement of the Soil at the Pit Bottom and above the Pit Bottom

**Figure 7** Side Foundation Pit Support Structure Form

For the side foundation pit project within the protection area of the operating subway (within 50m), especially the sandy soil area where foundation pit precipitation is strictly prohibited, it is proposed to propose the foundation pit support control design concept of "early isolation, strong block, and soft pit". That is:

Early isolation: construct water-stop curtains as soon as possible on both sides of the operating subway, and it is

advisable to use retaining structure systems such as ground-connected walls and cast-in-place piles. The water-stop curtains should be continuously closed and the bottom should enter the weak permeable layer.

Strong block: The foundation pits on both sides of the operating subway should adopt a bored pile + mixing pile structure system with large overall stiffness for primary block division to strictly control the lateral displacement of the tunnel.

Soft pit division: Each block foundation pit should adopt a mixing pile retaining structure system with lower rigidity for secondary pit division, and supplemented by slope reduction, to improve the spatial combination effect of block foundation pit excavation.

Taking the foundation pit engineering of Hangzhou Convention and Exhibition Center project as the background, and based on the research conclusion of the relative position pre-control index of the side foundation pit, when the tunnel deformation limit is 15mm, the length of the small foundation pit is controlled within 50m.

TRD cement soil mixing wall + cast-in-place piles are used as water-stop curtains near the subway on the north side, and TRD plug-in steel cement soil mixing wall is used as water-stop curtains near the subway on the south side; the block foundation pit adopts mixing piles + bored piles double rows of strong enclosure; the single block foundation pit adopts double rows of cement mixing piles for further soft division. Based on the engineering background of the south and north area foundation pits with an east-west length of about 530m, the south side is divided into 8 blocks and 16 small foundation pits, and the north side is divided into 6 blocks and 12 small foundation pits.

Using three-dimensional finite element software, the impact of batch and block jump excavation of the side foundation pit on the adjacent tunnel is analyzed. Construction Conditions can be seen in Table 4 and Three-Dimensional Finite Element Model can be seen in Figure 8.

**Table 4** Construction Conditions

| | |
|---|---|
| Condition 1 | earthwork excavation and construction of bottom plate, dismantling of supports (South I-5 area, South I-6 area, South I-7 area, South I-8 area, North I-1 area, North I-2 area, North I-3 area) |
| Condition 2 | earthwork excavation and construction of bottom plate, dismantling of supports (Condition 1 top plate construction completed; South I-1 area, South I-2 area, South I-3 area, South I-4 area, North I-4 area, North I-5 area, North I-6 area and part of the II blocks on the north and south sides) |

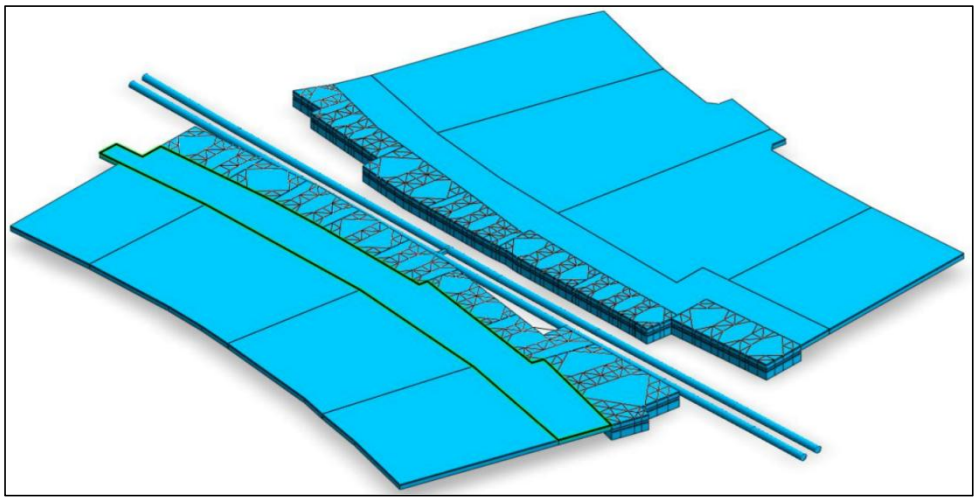

**Figure 8** Three-Dimensional Finite Element Model

Just as Figure 9 and 10, comparative analysis of calculation results:

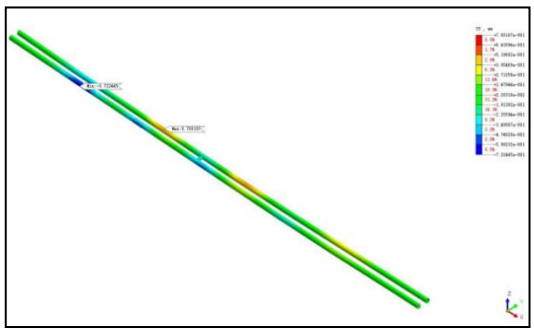

(a) Tunnel Horizontal Displacement

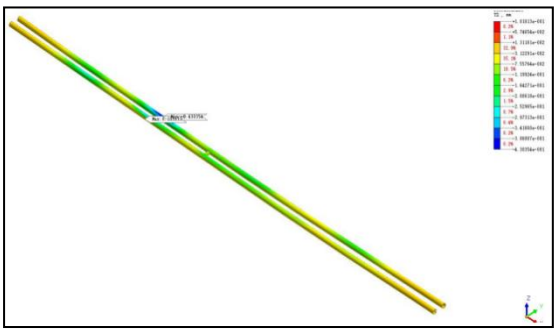

(b) Tunnel Vertical Displacement

**Figure 9** Condition 1: Earthwork Excavation and Construction of Bottom Plate, Dismantling of Supports

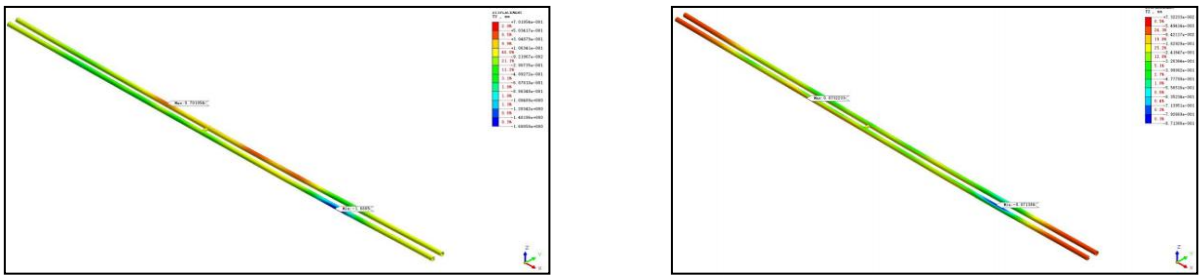

(a) Tunnel Horizontal Displacement (b) Tunnel Vertical Displacement

**Figure 10** Working Condition 2: Earthwork Excavation and Construction of Bottom Plate, Support Removal

The horizontal displacement of the tunnel caused by working condition 1: -0.72mm, and the vertical displacement: 0.43mm;

The horizontal displacement of the tunnel caused by working condition 2: earthwork excavation and construction of bottom plate, support removal: -1.68mm, and the vertical displacement: 0.87mm.

When the tunnel deformation limit is 15mm, the length of the small foundation pit is controlled within 50m, and combined with the foundation pit support control design concept of "early isolation, strong block, soft pit", the calculated horizontal and vertical displacements of the tunnel did not exceed the deformation limit, which further verified the rationality of the concept.

## 4 CONCLUSION

Taking the Hangzhou Convention and Exhibition Center project as an example, this study proposed a support control method based on micro-disturbance pre-control technology for the difficulties in the construction of long and deep foundation pits next to the operating subway. By constructing a deformation prediction function, a reasonable excavation length control standard is formulated, and the support design concept of "early isolation, strong block, soft pit" is proposed, and its effectiveness is verified by combining three-dimensional finite element analysis. The research results show that the pre-control technology can effectively control the disturbance of foundation pit construction to the subway tunnel and ensure the structural safety of subway operation. Future research can further optimize the pre-control model and apply and promote it in more practical projects.

## COMPETING INTERESTS

The authors have no relevant financial or non-financial interests to disclose.

## REFERENCES

[1] Zhang Jiantao, Yao Aijun, Guo Haifeng, et al. Analysis of the influence of unloading and loading of adjacent foundation pit on existing soft soil shield tunnel. Tunnel Construction, 2016, 36(11): 1348-1355.

[2] Yuan Zhao. The influence of deep foundation pit on adjacent subway stations and shield tunnels. Journal of Zhejiang Institute of Water Resources and Hydropower, 2017, 29(02): 53-60.

[3] Huang Pei, Chen Hua, Zhang Qian. The influence of large foundation pit zoning excavation on adjacent subways. Engineering Investigation, 2015, 43(08): 15-20.

[4] Zhang Jiao, Wang Weidong, Li Jing, et al. Three-dimensional finite element analysis of the influence of zoned construction pit on the deformation of adjacent tunnels. Building Structure, 2017, 47(02): 90-95. DOI:10.19701/j.jzjg.2017.02.017.

[5] Qiu Peiyun, Qi Yuliang, Chen Shuaiguang. Analysis of the influence of the foundation pit construction of a subway station in Guangzhou on the adjacent existing subway stations and tunnels. Guangdong Civil Engineering and Architecture, 2018, 25(03): 47-49+70.

[6] Wang Weidong, Shen Jian, Weng Qiping, et al. Analysis and countermeasures of the influence of foundation pit engineering on adjacent subway tunnels .Chinese Journal of Geotechnical Engineering, 2006, (S1): 1340-1345.

[7] Wang Lifeng, Pang Jin, Xu Yunfu, et al. Study on the influence of foundation pit excavation on adjacent operating subway tunnels. Rock and Soil Mechanics, 2016, 37(07): 2004-2010. DOI: 10.16285/j.rsm.2016.07.022.

[8] Jiang Hongsheng, Hou Xueyuan. The influence of foundation pit excavation on adjacent soft soil subway tunnels. Industrial Construction, 2002, (05): 53-56.

[9] Xiao Tonggang. Effect of foundation pit excavation construction monitoring on adjacent subway tunnels Analysis of the influence of foundation pit construction on the deformation of operating subway tunnels. Chinese Journal of Underground Space and Engineering, 2011, 7(05): 1013-1017.

[10] Gao Guangyun, Gao Meng, Yang Chengbin, et al. Study on the influence and control of foundation pit construction on the deformation of operating subway tunnels. Chinese Journal of Geotechnical Engineering, 2010, 32(03): 453-459.

[11] Ma Qiang. Design and practice of deep foundation pit engineering adjacent to subway tunnels. Green and Environmentally Friendly Building Materials, 2018, (04): 85. DOI:10.16767/j.cnki.10-1213/tu.2018.04.07 4.
[12] Yan Jingya. A brief discussion on the design and construction of deep foundation pits adjacent to operating subway tunnels. Chinese Journal of Geotechnical Engineering, 2010, 32(S1): 234-237.
[13] Liu Xiong. Analysis of deep foundation pit excavation adjacent to subway tunnels. Fujian Building Materials, 2021, (08): 59-61.
[14] Yin Yingzi, Liu Bin. Monitoring and analysis of deep foundation pit excavation adjacent to existing subway tunnels. Construction Technology, 2016, 47(09): 85-787. DOI:10.13731/j.issn.1000-4726.2016 .09.004.
[15] Kuang Longchuan. Impact of deep foundation pit construction on subway tunnels. Chinese Journal of Geotechnical Engineering, 2000, (03): 284-288.
[16] Dai Bohong. Prediction of the impact of deep foundation pit construction on adjacent subway tunnels. Urban Rail Transit Research, 2008, (08): 62-65.
[17] Xue Yongshen, Huang Yulin. Zoning construction technology of deep and large foundation pits in soft soil under complex environment. Shanghai Construction Technology, 2014, (01): 36-39.
[18] Wang Hang. Analysis of the impact of adjacent construction of building foundation pits on subway shield tunnels . China Standardization, 2017, (12): 238-240.
[19] Wang Hang. Analysis of the influence of foundation pit construction on subway shield tunnel section. Geotechnical Foundation, 2019, 33(01): 19-22.
[20] Huang Xun, Shi Li, Jin Lei, et al. Influence of long strip foundation pit construction on soft soil foundation on deformation of existing adjacent tunnels. Journal of Zhejiang University of Technology, 2020, 48(03): 261-268+299.
[21] Zheng Gang, Du Yiming, Diao Yu, et al. Study on the influence zone of deformation of adjacent existing tunnels caused by foundation pit excavation. Geotechnical Engineering Journal of Zhejiang University, 2016, 38(04): 599-612.
[22] Wen Zhongyi, Zhang Lijuan, Chen Song, et al. Study on the influence of foundation pit support structure deformation on adjacent subway tunnels. Roadbed Engineering, 2014, (05): 144-148. DOI: 10.13379/j.issn.1003-8825.2014.05.31.
[23] Chen Renpeng, Meng Fanyan, Li Zhongchao, et al. Excessive displacement of subway tunnels adjacent to deep foundation pits and protection measures. Journal of Zhejiang University (Engineering Science), 2016, 50(05): 856-863.

**World Journal of Engineering Research**
**ISSN: 2959-9873**
**DOI: https://doi.org/10.61784/wjer3005**

# STUDY ON THE PERFORMANCE OF LARGE-SPAN STEEL STRUCTURE OF DOUBLE-LAYER EXHIBITION HALL

Xing Gao[1,2], ZhiCheng Bai[1,2*], Yi Zhu[1,2], MinRong Shi[1,2], HuiZhou Ni[1,2]
*[1]China Construction Fourth Engineering Bureau Co., Ltd. Guangzhou 51000, Guangdong, China.*
*[2]China Construction Fourth Engineering Bureau Sixth Construction Co., Ltd. Hefei 230000, Anhui, China.*
*Corresponding author: ZhiCheng Bai, Email: 19822660870@163.com*

**Abstract:** This paper systematically studies the performance of large-span steel structure of double-layer exhibition halls 6# and 7# of Hangzhou Convention and Exhibition Center. Through detailed analysis of the structural system, material selection, node design and seismic performance of the exhibition hall, its structural performance under large span and heavy load conditions was evaluated. The research results show that the steel frame and floor truss structure system adopted in the double-layer exhibition hall not only ensures stability and bearing capacity, but also reflects the advantages of green building and prefabricated building. Finite element analysis verifies the safety and durability of the structure, providing an important reference for the design and construction of similar large-span exhibition buildings in the future.

**Keywords:** Large-span steel structure; Double-layer exhibition hall; Seismic performance; Node analysis

## 1 INTRODUCTION

With the development of economic globalization and the rapid rise of the exhibition economy, high-level exhibition infrastructure has become an important manifestation of urban competitiveness [1-3]. As an important exhibition venue in Hangzhou, the design of the 6# and 7# double-layer exhibition halls of the Hangzhou Convention and Exhibition Center must not only meet the needs of large-scale exhibition activities, but also ensure the safety and economy of the structure under large span and heavy load conditions. This paper aims to analyze the structural characteristics and performance of the large-span steel structure of the double-layer exhibition hall through in-depth research, and provide theoretical and practical support for similar projects in the future.

## 2 PROJECT OVERVIEW

The Hangzhou Convention and Exhibition Center is located in Nanyang Street, Xiaoshan District, Hangzhou City. The building area is about 740,000 square meters and the total construction area is 1.34 million square meters. The volume ranks first in Zhejiang Province and fifth in the country. Among them, the exhibition halls 6# and 7# of the Convention and Exhibition Center are precisely double-layer steel structures, with a length of 222 meters, a width of 104 meters, a building height of about 42 meters, and a roof elevation of about 19 meters. The main structural system includes a combination of steel frames and layer trusses, and the roof is a triangular space truss structure, which can effectively bear the above-mentioned loads of the building which can be seen in Figure 1.

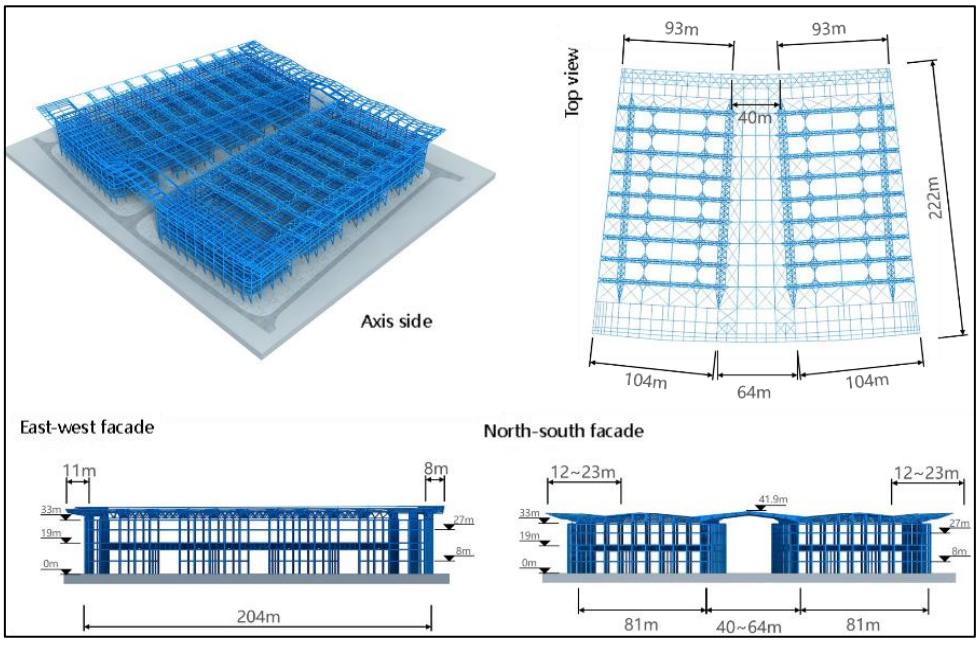

**Figure 1** Overview of Double-Layer Steel Structure Exhibition Halls

## 3 CURRENT STATUS OF EXHIBITION HALL FLOOR SYSTEMS AT HOME AND ABROAD

By comparing the characteristics of large-span, heavy-load floor slabs and structural systems of domestic exhibition buildings, the following table 1 shows some existing double-layer or multi-layer exhibition hall floor slab systems in China. The results show that the floor span is in the range of 20-30m, and the structural form is mainly prestressed concrete floor slabs and steel trusses + concrete floor slabs.

**Table 1** Floor System of Domestic Exhibition Buildings

| No. | Projects | Column grid/m | Floor height/m | Floor system |
|---|---|---|---|---|
| 1 | Guangdong Modern International Exhibition Center | 30×21 | 12 | prestressed |
| 2 | Guangzhou International Convention and Exhibition Center | 24×24 | 10 | prestressed |
| 3 | Wuhan International Convention and Exhibition Center | 32×17 | - | prestressed |
| 4 | Hongdao International Convention and Exhibition Center | 36×24 | 14.7 | prestressed |
| 5 | National Convention and Exhibition Center (Shanghai) | 36×27 | 16 | prestressed |
| 6 | Jinan International Convention and Exhibition Center | 24×24 | 10 | prestressed |
| 7 | Hunan International Convention and Exhibition Center | 21×21 | 12 | prestressed |
| 8 | Shandong Lutai Convention and Exhibition Center | 27×24 | 16 | steel truss |
| 9 | Hangzhou International Expo Center | 36×27 | 16 | steel truss |

From the perspective of overall cost, the material cost of prestressed concrete floor is lower than that of steel truss floor, but considering the current national industrial policy of vigorously developing green buildings and prefabricated buildings, steel structure is obviously a more suitable structural form for the current main development trend. Comparison of Advantages and Disadvantages of Floor Forms can be seen in table 2.

**Table 2** Comparison of Advantages and Disadvantages of Floor Forms

| No. | Comparison content | Floor type | |
|---|---|---|---|
| | | Steel truss floor | Prestressed concrete floor |
| 1 | Comprehensive cost | 3500-3800 Yuan/$m^2$ | 2700-3300 Yuan/$m^2$ |
| 2 | Green energy saving | Meet the requirements of green building, the main materials are renewable | Does not meet green building requirements |
| 3 | Prefabricated | Meet the requirements of prefabricated steel structure | Does not meet prefabricated building requirements |
| 4 | Construction speed and difficulty | Steel structure is directly assembled, and the construction is fast. The floor truss and steel beams directly form rigidity, and the floor deck can be laid directly without formwork | Concrete structures require high formwork scaffolding, and it is difficult to bury corrugated pipes on site for prestressing and post-tensioning |
| 5 | Structural deadweight | Light weight, small earthquake response | Heavy deadweight, large earthquake response |
| 6 | Clear height | The space of the truss web can be used to arrange mechanical and electrical pipelines and maintenance horseways, which is beneficial to the clear height | Solid cross-section, pipelines need to run under the beam |

## 4 FLOOR STRUCTURE ANALYSIS

### 4.1 Main and Secondary Trusses

The second floor of the double-layer exhibition hall is 81m east-west and 174m north-south; the east-west column span spacing is 27m, and the north-south column span spacing is 36m. The structural model is as shown below figure 2.

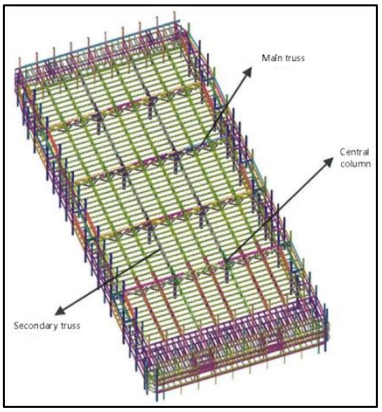


**Figure 2** Double-Layer Exhibition Hall Floor Structure Model

Taking into account the secondary beam span, truss spacing and other factors, 4 3-span continuous main trusses are set in the east-west direction, with a span of 27m, supported on steel columns. There are 8 secondary trusses in the north-south direction, with a spacing of 9m, supported on steel columns or main trusses. Considering that there is still a need to pass through the horseway and large smoke exhaust pipes between the trusses, the center spacing between the upper and lower chords of the truss is 4.0m. Due to the large overall shear force at the truss support, the web members are arranged in a cross X shape, and in the middle of the truss, the web members are arranged in an inverted V shape to facilitate the passage of the horseway and pipelines. In order to reduce the inter-section distance of the upper chord of the secondary truss, a vertical web member is set every 6m. The truss elevation is shown in the figure 3 and 4 below.

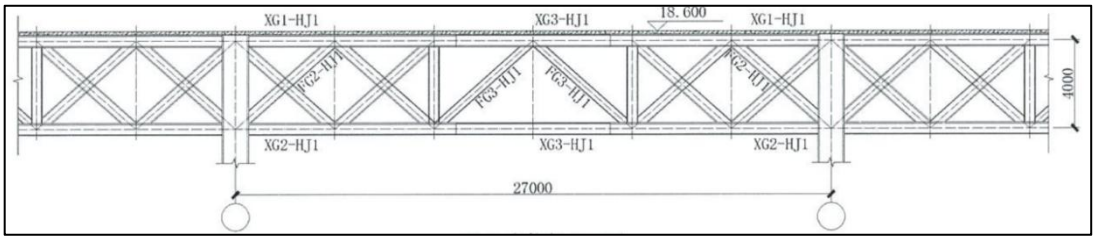


**Figure 3** Main Truss Elevation

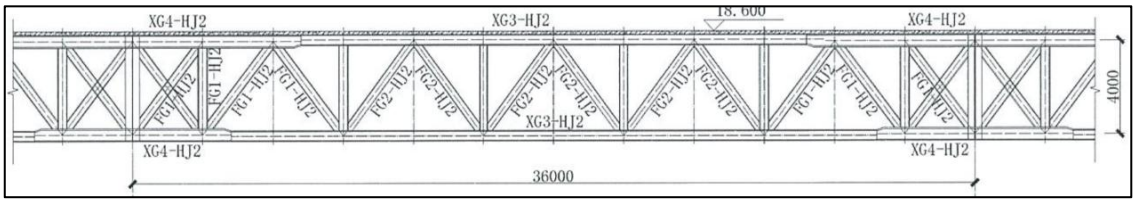


**Figure 4** Secondary Truss Elevation

The truss is calculated as a whole using finite element software, and the components are inspected according to the corresponding specifications and design criteria. After empirical calculation, the maximum stress ratio of the components at the truss support is 0.91<1. The stress ratio of most members is controlled below 0.70. Taking into account the factors such as the type of cross-section of the truss members and making full use of the stress of the members, different chord and web sections are used for the support and the mid-span according to the stress section, taking into account the processing difficulty and the balance of the structural cost. The calculation results of the truss deformation are shown in the following table 3. The truss meets the corresponding deformation requirements of the specification under the action of live load and dead load + live load.

**Table 3** Calculation Results of Truss Deformation

| Loading conditions | Dead load + live load | Live load |
|---|---|---|
| Main truss deformation | 35mm（1/771） | 18mm（1/1500） |
| Secondary truss deformation | 73mm（1/493） | 37mm（1/972） |
| Deformation limit | 1/400 | 1/500 |

### 4.2 Floor Secondary Beam

The live load of the second-floor exhibition hall floor is 15kN/m2. If the plate thickness is 150mm, then combined with the plane column grid modulus and the inter-node distance of the secondary frame, the 3m plate span is more reasonable. The floor slab adopts TD3 steel truss floor slab, in which the height of the steel truss is 120mm. The secondary beam

section adopts welded H-shaped steel H600×350×12×20, with a span of 9m, and both ends are hinged to the secondary truss. The calculation results show that the maximum stress ratio of the component strength verification is 0.98. Because the rigid concrete floor is laid on the upper part of the secondary beam, the overall stability of the steel beam can be ignored. The repetition rate of the secondary beam on the floor is very high, and the steel consumption accounts for about 20% of the entire truss floor. As shown in table 4, by setting two rows of Φ19@200 bolts on the upper flange of the secondary beam to cooperate with the upper concrete floor slab to form a composite beam, the overall steel consumption is effectively reduced, and the maximum stress ratio of the secondary beam is reduced to 0.6.

**Table 4** Slab Span-Load

| Plate thickness/mm | Board span/m | | |
|---|---|---|---|
| | Use live load 10-11kN/m$^2$ | Use live load 12-13kN/m$^2$ | Use live load 14-15kN/m$^2$ |
| 150 | 4.2-4.5 | 3.9-4.2 | 3.3-3.5 |
| 180 | 5.0-5.5 | 4.5-5.0 | 4.0-4.5 |

## 5 STRUCTURAL CALCULATION AND ANALYSIS

Since the steel roof structure of the double-layer and single-layer exhibition halls is the same, the single-layer exhibition hall is taken as an example to focus on the stress performance of the large-span steel roof structure. The roof of the exhibition hall is fan-shaped when viewed from above and folded line-shaped when viewed from the facade. It is a light steel roof system. Plane trusses are used in the cantilevered area outside the column. The change from two upper chords to one upper chord is completed at the steel column of the exhibition hall, and the lower chord bending point of the truss in the cantilevered area is set within the curtain wall line to minimize the height of the truss in the cantilevered area. A connecting truss and a cross steel tie rod are set between each truss, which not only enhances the integrity of the roof structure, but also serves as a force transmission path perpendicular to the span direction of the truss, and plays a role in lateral support for the main truss.

The upper and lower chords and webs of the main truss are all round tubes, with a material grade of Q355, and the main cross-section is 500×20 for the upper chord, 800×30 for the lower chord, and 245×8 for the web; the secondary chord is Φ351×12, and the web is Φ203×8; the steel column is Φ1200×40. The upper chord of each truss is in a broken line shape on the facade, which fits the design concept of the building. The truss section and side view are shown in the figure 5 and 6 below.

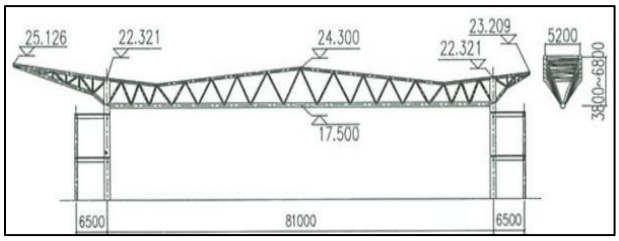


**Figure 5** Main truss section

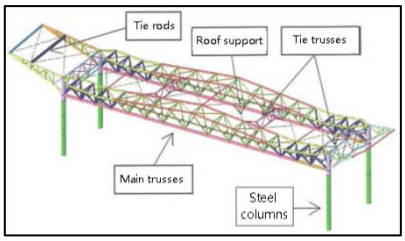


**Figure 6** Main truss axonometric view

The finite element method is used to model, calculate and analyze the steel structure roof of the exhibition hall, and the three-dimensional calculation model is shown in the figure 7 below.

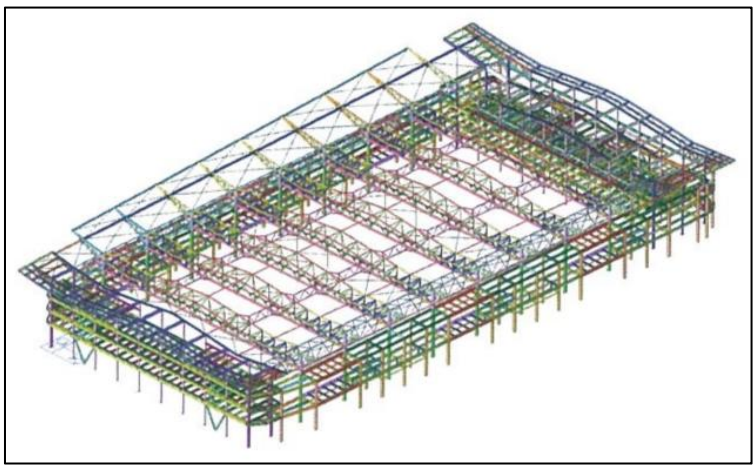

**Figure 7** 3D Calculation Model of the Exhibition Hall

### 5.1 Self-Vibration Analysis

In table 5, by performing eigenvalue analysis on the exhibition hall, the first ten vibration modes of the structure are obtained, and the first three vibration modes are shown in the figure 8-10 below. From the vibration mode results, it can be seen that the exhibition hall structure has good integrity and uniform stiffness distribution, which meets the requirements of the period ratio.

**Table 5** Natural Vibration Period of the Exhibition Hall Structure

| Mode | Period/s | Translation coefficient（X+Y） | Torsion coefficient |
|---|---|---|---|
| 1 | 1.3938 | 1.00(0.00+1.00) | 0.00 |
| 2 | 1.2316 | 0.95(0.95+0.00) | 0.05 |
| 3 | 1.1421 | 0.04(0.04+0.00) | 0.96 |
| 4 | 1.1223 | 0.94(0.06+0.88) | 0.06 |
| 5 | 1.1040 | 0.24(0.24+0.00) | 0.76 |
| 6 | 1.0292 | 0.84(0.84+0.00) | 0.16 |
| 7 | 1.0154 | 0.85(0.08+0.77) | 0.15 |
| 8 | 1.0008 | 0.50(0.11+0.39) | 0.50 |
| 9 | 0.9478 | 0.31(0.15+0.16) | 0.69 |
| 10 | 0.9317 | 0.47(0.47+0.00) | 0.53 |

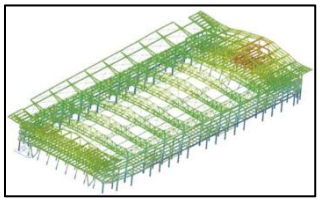

**Figure 8** First-Order Translation (1.3938s)

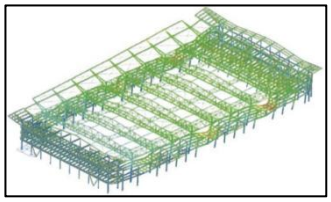

**Figure 9** Second-Order Translation (1.2316s)

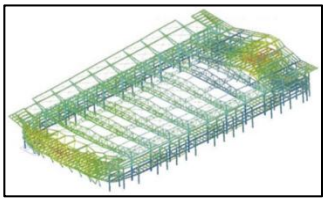

**Figure 10** Third-Order Translation (1.1421s)

### 5.2 Deflection Analysis

The maximum roof deflection of the exhibition hall roof under the standard values of dead load and live load is 165mm, which occurs in the span, as shown in the figure 11-13 below. The arch is 100mm in the span of the truss, and the actual deflection-span ratio is: (165-100)/81000=1/1246<1/400.

The maximum roof deflection of the exhibition hall roof under the standard value of live load is 61mm, located in the middle of the truss span, see Figure 7 for details. The actual deflection-span ratio is: 61/81000=1/1327<1/500.

The maximum roof deflection of the exhibition hall roof under the representative value of gravity load and the standard value of multiple vertical earthquake action is 141mm, see the figure below for details. The actual deflection-span ratio is: 141/81000=1/575<1/250.

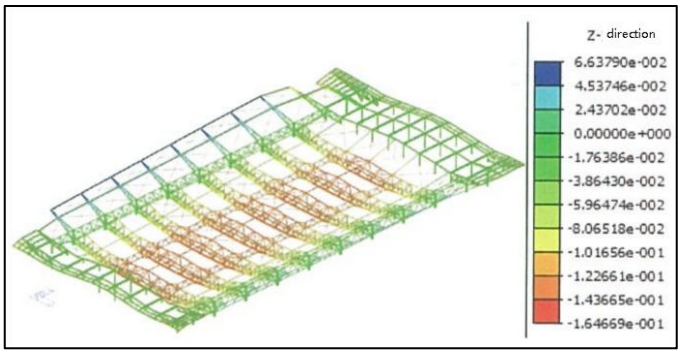


**Figure 11** Vertical displacement Contour of Roof Structure under Standard Constant + Live Load

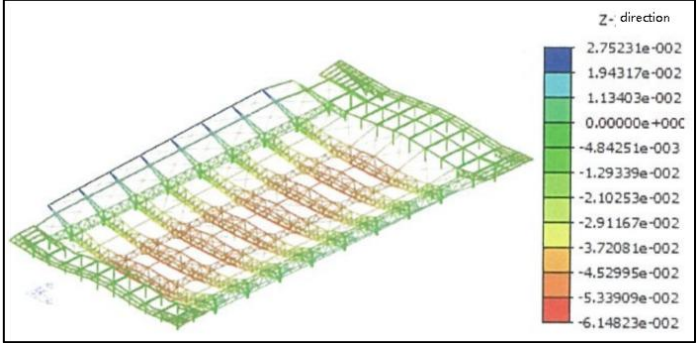


**Figure 12** Vertical Displacement Contour of Roof Structure under Standard Live Load

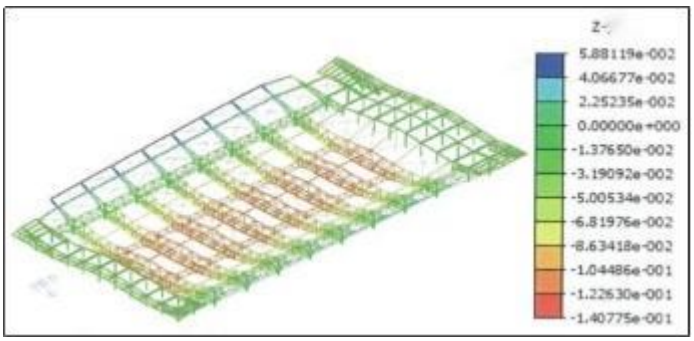


**Figure 13** Vertical Displacement Contour of Roof Structure under Representative Value of Gravity Load and Standard Value of Multiple Vertical Earthquake Action

### 5.3 Seismic Performance Analysis

When considering moderate earthquakes, the seismic partial coefficient is taken as 1.0, and the component material partial coefficient is taken as 1.0. The figure 14 below is a stress ratio cloud diagram of steel columns and main truss members of the roof under moderate earthquake. It can be seen from the results that the steel columns and main truss members of the single-story exhibition hall are in an unyielding state, and the maximum stress ratio of the members is 0.96.

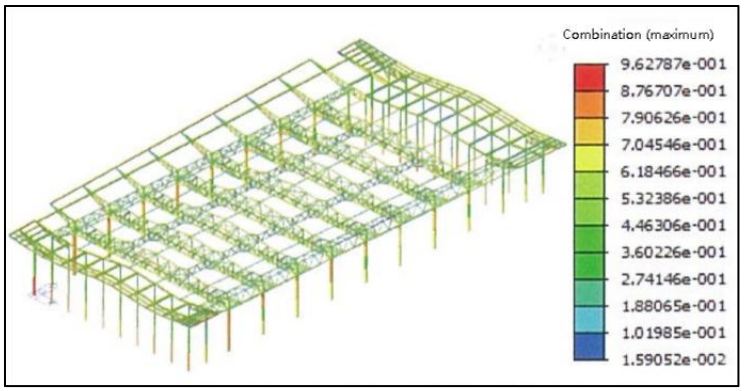


**Figure 14** Stress Ratio Cloud Diagram of the Roof Structure Members of the Single-Story Exhibition Hall under Moderate Earthquake

## 6 CALCULATION AND ANALYSIS OF COMPLEX NODES

By selecting two typical complex stress nodes, a refined finite element analysis is performed to improve and perfect the node structure. The ideal elastic-plastic model is used for the steel constitutive model, the elastic modulus E is 2.1×105MPa, and the Poisson's ratio v is 0.3; the yield strengths of the steel pipe and the tie rod are 355MPa and 460MPa respectively.

### 6.1 Typical Truss Intersection Node

The cross section of the steel tie rod is a Φ50 steel bar. The model uses the solid element C3D10M; the left end of the main pipe is fixedly constrained, and the remaining members are considered as free ends; a surface-to-surface contact is set between the tie rod pin and the connecting ear plate; the node load uses the most unfavorable load combination calculated by the overall model, and the members not only consider the axial force but also the influence of shear force and bending moment under the most unfavorable combination. The node stress distribution is shown in the figure 15 and 16 below. The maximum stress is about 284.11MPa, located at the intersection of the tie rod connecting plate and the chord, that is, the stress concentration area, and the node area remains in an elastic state.

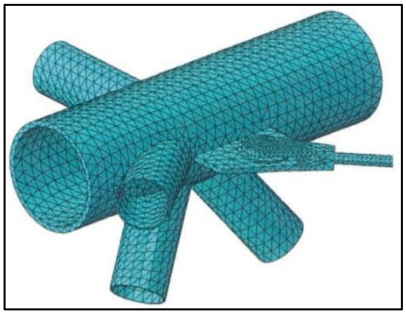

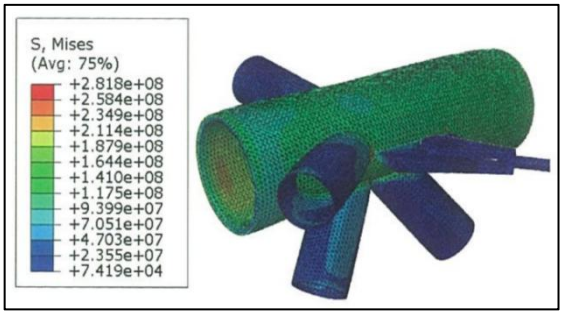

**Figure 15** Three-Dimensional Model of truss Intersection Node

**Figure 16** Stress Cloud Diagram of Truss Intersection Node

### 6.2 Roof Support Node

The column spacing of the roof structure between the double-layer exhibition halls is 40-64m. In order to avoid exceeding the length limit, brackets are set on the top of the exhibition hall frame columns, one end uses a fixed support and the other end uses a sliding support. The roof section and support details are as follows Figure17 and 18.

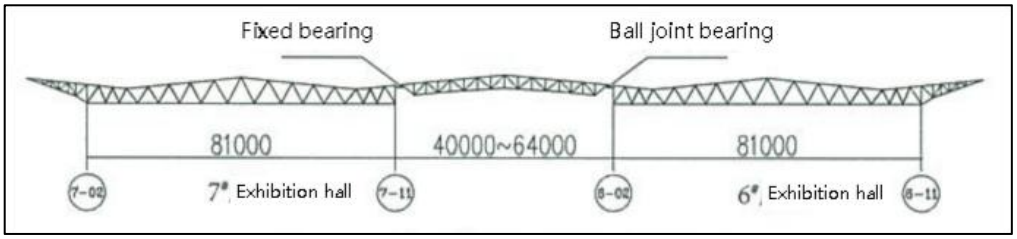


**Figure 17** Roof Section Of Double-Layer Exhibition Hall

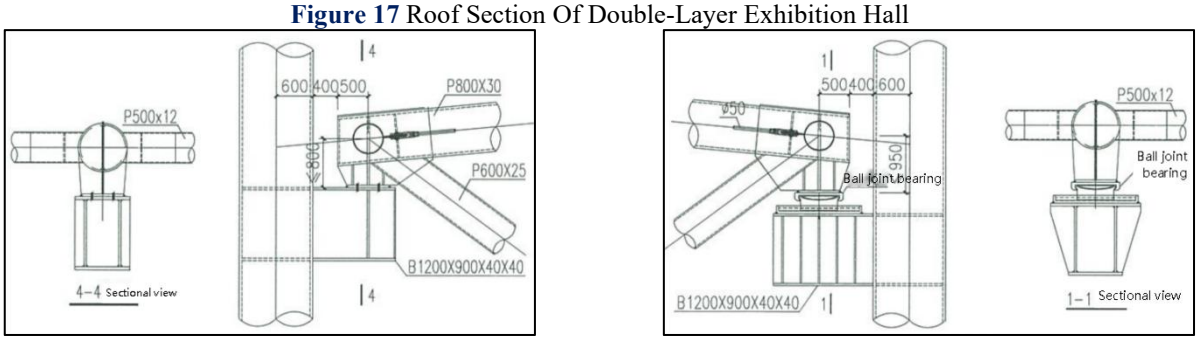


(a) Fixed End Support (b) Sliding End Support

**Figure 18** Support Node Details

The fixed support node has many rods, complex structure and large force on each rod, so a refined finite element analysis is performed on this node. The three-dimensional model of the node is shown in the figure 19 below. The model uses solid unit C3D10; the four sides of the bottom plate are fixedly constrained and the remaining rods are considered as free ends; the node load uses the most unfavorable load combination calculated by the overall model, and the rods not only consider the axial force but also the shear force and bending moment. The stress distribution of the support node under the most unfavorable load combination is shown in the figure 20below. Except for the local stress concentration, the stress in most areas of the node is less than 290MPa, and the support node is basically in an elastic state.

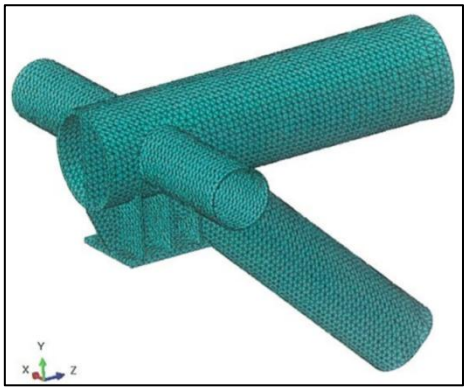

**Figure 19** Support Node Three-Dimensional Model

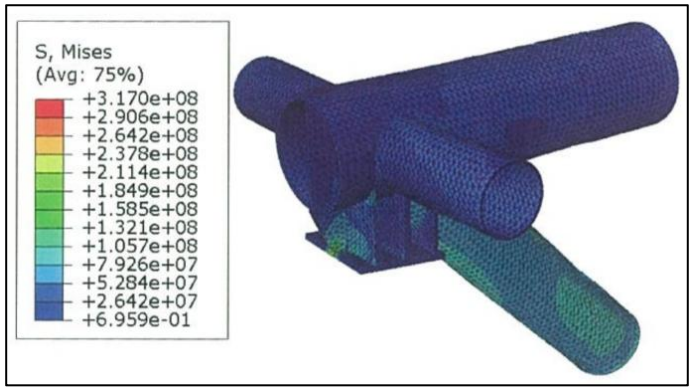


**Figure 20** Support Node Stress Cloud Diagram

Based on the above overall structure and main node simulation analysis, the overall performance of the exhibition hall roof structure is good and the stiffness is uniform. However, the main truss of the large span is subjected to greater force at the support, and the triangular three-dimensional truss is transformed into a plane truss at the support. It is necessary to appropriately strengthen the strength and stiffness of this place, and take measures to strengthen the stability of the plane truss in the cantilever area.

## 7 CONCLUSION

This paper systematically studies the performance of the large-span steel structure of the double-layer exhibition hall of the Hangzhou Convention and Exhibition Center. The study shows that the steel frame and truss structure system of the double-layer exhibition hall has excellent stability and bearing capacity under heavy load and large span conditions, and is in line with the development trend of green buildings and prefabricated buildings. Finite element analysis verifies the safety and reliability of the structure and nodes, and provides valuable experience and reference for the design and construction of similar large-span exhibition buildings in the future. The research results not only promote the engineering practice of the Hangzhou Convention and Exhibition Center, but also have important significance for the development and technological progress of my country's convention and exhibition construction industry.

## COMPETING INTERESTS

The authors have no relevant financial or non-financial interests to disclose.

## REFERENCES

[1] Ding Fengyao, Chen Zhaosheng, Jin Ping. Construction technology of large-span inverted triangle tube truss in Guilin New Exhibition Center. Building Structure, 2023, 53(S2): 1790-1794.
[2] Zhang Chenglong. Research on overall stability performance of double-layer cable-supported prestressed steel columns with cross cables. Chongqing University, 2020.
[3] Hu Yi. Construction technology of large-span steel truss roof for single- and double-layer combined exhibition halls. Building Construction, 2015, 37(08): 922-923.

**World Journal of Engineering Research**
**ISSN: 2959-9873**
**DOI: https://doi.org/10.61784/wjer3006**

# EFFECT OF FREQUENCY ON LOSSES IN A 77K MINIATURE PNEUMATIC STIRLING CRYOCOOLER

GengChen Liu[1*], AnKuo Zhang[1], Bo Yu[2], YangPing Zeng[2], Shu Wang[2]
*[1]Department of Refrigeration and Cryogenic Engineering, Shanghai Ocean University, Shanghai 201306, China.*
*[2]Cryocooler Development Department, Zhejiang JueXin Microelectronics Co, Ltd, Lishui 323000, Zhejiang, China.*
*Corresponding Author: GengChen Liu, Email: Gengchen-Liu@qq.com*

**Abstract:** This paper investigates the impact of frequency on the losses within a 77K miniature pneumatic Stirling cryocooler. Low-temperature cryocoolers are essential for providing a low-temperature working environment for high-performance cooled thermal imaging detectors. Stirling cryocoolers can achieve a higher relative Carnot efficiency under low heat load conditions. By establishing a one-dimensional numerical model and analyzing the mechanisms of various internal losses, this study examines the trends of internal energy loss within different components as a function of working frequency, ultimately determining the optimal frequency for the Stirling cryocooler. The results indicate that flow resistance loss, non-ideal heat transfer loss, axial conduction loss, and shuttle loss are the primary loss types in miniature pneumatic Stirling cryocoolers. Experimental testing and analysis confirm the accuracy of the numerical simulation results and demonstrate the performance of the cryocooler at different frequencies. The cryocooler can achieve a cooling capacity of 905 mW@77 K@ 24.2 $W_{in}$ at its optimal operating condition. This study provides a theoretical basis and experimental support for the design and optimization of miniature Stirling cryocoolers.
**Keywords:** Stirling cryocooler; Frequency; Losses; Effect; Pneumatic; Mid-wave infrared detector

## 1 INTRODUCTION

Low-temperature cryocoolers play a crucial role in providing a low-temperature working environment for high-performance cooling-type thermal imaging detectors. For lower thermal noise, typical mid-wave infrared cooling detectors need to operate within a low-temperature range of 70-80 K, which allows them to achieve higher temperature sensitivity, greater measurement distance, and higher spatial resolution compared to non-cooling detectors [1–4]. However, cooling detectors have higher costs, larger sizes, and higher power consumption, which sets higher demands for the cryocooler.

Under low heat load conditions, Stirling cryocoolers can achieve a higher relative Carnot efficiency compared to other types of cryocoolers. The widespread application of linear compressors has greatly enhanced the operational lifespan of pneumatic Stirling cryocoolers compared to rotary Stirling cryocoolers, while significantly reducing the overall size and vibration[5–7]. Therefore, miniature pneumatic Stirling cryocoolers, characterized by small size, long life, low vibration, high refrigeration efficiency, and low weight, can meet the current infrared requirements.

For pneumatic Stirling cryocoolers, the compressor and expander can each be regarded as a vibration system. If their natural frequencies are matched, the cryocooler will be in a resonant state, and operating at the resonant frequency allows for the highest cooling capacity with the least electrical work input. Thus, adjusting the cooling performance and the matching relationship between the expander and compressor can be achieved by varying the operating frequency to find the cryocooler's resonant frequency. During the engineering development process, it is necessary to determine the impact of frequency on the internal energy loss distribution and refrigeration performance of the entire machine to ascertain the cryocooler's resonant frequency.

Over several decades, Thales has developed numerous models of Stirling cryocoolers, including linear split types such as the UP708x, UP8xxx, LSF93xx, LSF95xx, and LSF99xx series[8,9]. Consequently, they have initiated improvements to the previously developed LSF93xx and LSF95xx models to extend their service life. Optimization strategies can be approached from two aspects: internal structure and operational parameters. The optimization plan for the LSF9340/50-HA models focuses on operational characteristics, specifically the detailed determination of operating frequency and filling pressure [10]. Ricor, a renowned manufacturer in the field of infrared cryogenics, offers products that are quite representative[11]. The K527S is a short cold finger type miniature linear split Stirling cryocooler[12]. The cold finger has been shortened from the original 44 mm to 19 mm, and the corresponding resonant frequency has increased from 68 Hz to 90 Hz. This indicates that there is an interaction between the structure of the regenerator and the resonance frequency. Cryotech Co, Ltd focuses primarily on the development of low-cost HOT miniature Stirling cryocoolers. The best operating frequency for their split cryocoolers is 80 Hz, with a filling pressure of 1 MPa, and they can achieve a cooling performance of 260 mW@150 K@1.6 $W_{ac}$[13,14].

From actual manufacturer products, it has been observed that there is a correlation between the structure and materials of the cryocooler and the resonant frequency. Changes in structure and materials will inevitably affect the distribution of internal losses; hence, a connection between losses and resonant frequency is inevitable. Currently, numerous studies involve the analysis of energy flow within the regenerator. From a theoretical standpoint, the cryocooler operates on the inverse cycle of a heat engine, which makes the study of heat engines valuable for the development and optimization of

cryocoolers M.T. Mabrouk et al.[15] derived the energy flow in the gaps of a β-type heat engine, analyzing the impact of gap width on loss conditions. Ruijie Li et al.[16] discussed theoretical or empirical formulas for various losses in Stirling heat engines and optimized the heat engine using the Finite Physical Dimensions Thermodynamics (FPDT) method based on multi-objective criteria. For Stirling heat engines, the GPU-3 modeling approach is widely adopted to study the dynamic characteristics of the engine. Although this method includes the mathematical construction of losses, the focus in engineering is on the entire cycle process and the final cycle efficiency, with less quantitative analysis of losses[17,18]. Swift [19]regarded thermoacoustic theory as a unified perspective for regenerative oscillating heat engines, including cryocoolers. Wang[20,21] elucidated the relationship between electromechanical-acoustics from the perspective of phase coupling. Most studies on cryocoolers are based on empirical formulas and theoretical derivations, using cooling capacity or cooling efficiency as optimization targets to analyze the performance of heat engines or cryocoolers[22]. Therefore, direct attention to the distribution of internal losses within a cryocooler is relatively scarce.
This paper aims to design and develop a 0.5W@77 K miniature split Stirling cryocooler, establishing a one-dimensional numerical model and analyzing the mechanisms of various internal losses. Further research is conducted from the perspective of energy loss to study the impact trends of working frequency on the internal energy loss of different components, ultimately determining the optimal frequency for this Stirling cryocooler.

## 2 LOSS TYPES IN MINIATURE PNEUMATIC STIRLING CRYOCOOLERS

A higher coefficient of performance (COP) indicates a more efficient and effective refrigerator. The factors affecting COP are the irreversible loss due to the flow resistance of the viscous working medium and the entropy generated by the conduction between the working medium and the wall surface. In general, irreversible loss can be divided into non-ideal heat transfer loss, flow resistance loss, conduction loss and shuttle loss[23]. Therefore, the study of the mechanism of irreversible loss can fundamentally weaken or avoid the loss, which will contribute to the optimization of the refrigerator.

### 2.1 Non-ideal Heat Transfer Losses

During the operation of a cryocooler, the flowing gas undergoes heat exchange with the original cavity gas, the heat sink wire mesh, and the walls. However, due to imperfect thermal dynamics, complete and effective heat exchange often cannot be achieved, leading to energy loss known as non-ideal heat transfer losses [24]. The majority of these losses occur within the regenerator.
The performance of a regenerator is typically assessed by its heat exchange efficiency, which can be simply represented as the ratio of actual heat transfer to the ideal heat transfer under specified design and operating conditions. As one of the key components in a Stirling cryocooler, the quality of the regenerator's performance dictates the ultimate performance of the cryocooler. The regenerator, being a type of heat exchanger, can have its efficiency defined using the number of transfer units (NTU)[25]:

$$\varepsilon = \frac{NTU}{NTU + 2} \tag{1}$$

$$NTU = \frac{A_{wetted} h}{\dot{m}_{ave,r} C_p} \tag{2}$$

where $A_{wetted}$ represents the wetted surface area involved in heat transfer within the regenerator, $\dot{m}_{ave,r}$ represents the average mass flow rate through the regenerator, $C_p$ represents the specific heat capacity at constant pressure of the working gas, and $h$ represents the heat transfer coefficient, given by the equation[26],

$$h = \frac{Nu\lambda_g}{D_r} = \frac{\lambda_g}{D_r} C_1 (\mathrm{Re}_{ave} Pr)^{C_2} \tag{3}$$

In the equation, $\lambda_g$ represents the thermal conductivity of the working gas, $C_1$ and $C_2$ are the empirical coefficients ($C_1 = 0.42$, $C_2 = 0.67$), $D_r$ represents the diameter of the regenerator, and $\mathrm{Re}_{ave}$ represents the average Reynolds number, $Pr$ represents the Prandtl number.

Therefore, the non-ideal heat transfer loss ($\dot{Q}_r$) is defined as:

$$\dot{Q}_r = \dot{m}_{ave,r} C_p (1 - \varepsilon) (T_H - T_C) \tag{4}$$

where $T_H$ and $T_C$ are the temperatures at the hot end and the cold end, respectively.
In practical applications, the regenerator is often designed with a matrix of wire mesh or porous material that provides a large surface area for heat transfer while allowing the working gas to flow through with minimal resistance. The choice of material, its porosity, and the geometric configuration are critical factors that influence the regenerator's ability to facilitate heat exchange without excessive energy loss.

### 2.2 Flow Resistance Losses

The working gas in a Stirling cryocooler passes through the regenerator and various pipes, and due to its own viscosity and the roughness of the walls, it generates flow resistance, leading to a decrease in pressure amplitude and thus a loss of cooling capacity. This type of loss is referred to as flow resistance loss. The flow resistance loss is caused by the reduction of expansion work in the cold space due to gas pressure drop, and the average flow resistance loss can be defined as the reduced expansion work [23,27]. And the formula is as follows:

$$\dot{Q}_{ave,fr} = \frac{1}{t}\int_0^t \Delta p_r(t)\,dV(t) \tag{5}$$

$$\Delta p_r(t) = \Delta p_{r,\max}\cos(\omega t) \tag{6}$$

$$\Delta p_{r,\max} = \frac{f_r \rho l_r U^2}{2D_r} \tag{7}$$

In the formula, $t$ represents a running cycle, $f_r$ represents the Fanning friction coefficient, $\rho$ represents the gas density, $U$ represents the axial gas flow velocity amplitude.

According to the experimental testing by Gedeon and Wood [28], the Fanning friction factor is related to the Reynolds number, , and the following formula exists:

$$f_r = 129\,\mathrm{Re}^{-1} + 2.91\,\mathrm{Re}^{-0.103} \tag{8}$$

### 2.3 Shuttle Losses

The displacer in a Stirling cryocooler plays a crucial role in exchanging the working gas between the compression space and the expansion space, while also maintaining a relatively constant temperature difference between the two working spaces. As the displacer moves towards the hot end from the center of its stroke, its surface temperature is lower than that of the cylinder wall at the same axial position. Consequently, heat is transferred from the cylinder to the displacer. Similarly, as the displacer moves towards the cold end, its surface temperature is higher, transferring heat from the displacer to the cylinder. Due to the thermal capacity of the displacer's surface, the temperature oscillation of the displacer is out of phase with its motion[29,30]. At a certain axial position, the enthalpy flow accompanying the displacer's motion in the cold direction is always greater than that in the hot direction. The net enthalpy flow rate from the hot region to the cold region is referred to as the shuttle heat, resulting in shuttle heat loss, which can be calculated using the following formula [31]:

$$\dot{Q}_{shuttle} = \frac{\pi D_r S}{4} 2\pi f \lambda \rho c T_{10} \tag{9}$$

$$T_{10} = \Gamma S \frac{a_2}{\sqrt{\left(\frac{a_1+a_2}{\sqrt{2}}\right)^2 + \left(\frac{a_1+a_2}{\sqrt{2}} + a_1 a_2\right)^2}} \tag{10}$$

In the formula, $S$ represents the stroke of the displacer, $f$ represents the operating frequency, $c$ represents the specific heat capacity, $\Gamma$ represents the temperature gradient,. The dimensionless numbers $a_1$ and $a_2$ are defined based on the characteristics of the space, heat transfer coefficient, and frequency, with the specific expression being:

$$a_1 = \frac{k_1}{h'}\sqrt{\frac{2\pi f}{\alpha_1}} \tag{11}$$

$$a_2 = \frac{k_2}{h'}\sqrt{\frac{2\pi f}{\alpha_2}} \tag{12}$$

where $h'$ represents the heat transfer coefficient, $k_1$ and $k_2$ respectively represent the thermal conductivity of the displacer and cylinder, $\alpha_1$ and $\alpha_2$ respectively represent the thermal diffusivity of the displacer and cylinder.

### 2.4 Pumping Losses

In Stirling cryocoolers, the pressure within the working space varies cyclically, leading to the presence of gas in the clearance between the displacer and the cylinder wall that either originates from or flows into the expansion space. This gas can absorb and transfer energy from the surrounding walls. Specifically, when the system pressure increases, the gas pressure within the clearance is lower than that in the expansion space, allowing a small amount of cold gas to enter the clearance from the expansion space and absorb heat from the displacer and cylinder walls, as well as from the initially present gas within the clearance[32]. Conversely, when the system pressure decreases, the gas pressure within the clearance becomes higher than in the expansion space, causing the gas to flow back into the expansion space. Due to non-ideal heat transfer between the gas and the displacer and cylinder walls, the temperature of the gas flowing into the

expansion space is higher than the space's temperature, resulting in heat release to the expansion space and an increased heat load at the cold end. This leads to a loss of cooling capacity for the cryocooler, known as pump gas loss[33,34]. The pump gas loss can be estimated using the following formula [35]:

$$\dot{Q}_{pump} = 4.04\,(T_H - T_C)\,\delta^{2.6}\left[\frac{fC_p}{RT_{ave}}\left(\frac{p_{\max}}{Z_H} - \frac{p_{\min}}{Z_C}\right)\right]^{1.6}\left(\frac{\pi D_r}{\lambda_g}\right)^{0.6} \tag{13}$$

### 2.5 Heat Conduction Losses

In a Stirling cryocooler, a significant temperature difference exists between compression space and the expansion space. Although they are separated by a regenerator, heat conduction cannot be ignored. The axial heat conduction losses through the regenerator matrix, cylinder walls, and wire mesh represent an additional thermal load on the regenerator. This loss is independent of the frequency and pressure of the refrigerator, and can be calculated according to Fourier's law of thermal conductivity [36,37], the specific formula is:

$$\dot{Q}_{cond,i} = k_i \frac{A_i}{l_i}(T_H - T_L) \tag{14}$$

In the given formula, $k_i$ represents the thermal conductivity of different components (regenerator shell, cylinder, wire mesh), $A_i$ represents the axial heat conduction cross-sectional area of different components, and $l_i$ represents the axial length of different components.

This loss is crucial to consider in the design and optimization of Stirling cryocoolers, as it impacts the overall efficiency and cooling performance of the system. Minimizing these conduction losses is essential for achieving higher coefficients of performance and better refrigeration capabilities, especially in applications requiring cryogenic temperatures for infrared detectors, superconducting magnets, and other sensitive instruments

## 3 NUMERICAL SIMULATION OF INTERNAL LOSSES IN MINIATURE PNEUMATIC STIRLING CRYOCOOLERS

As shown in Figure 1, a miniature pneumatic Stirling cryocooler can be divided into seven parts based on thermodynamic characteristics: the compression space, the secondary compression space, the compressor back pressure space, the expander back pressure space, the expansion space, the connecting tube, and the regenerator. Each of these parts needs to be discretized into many small and uniform sub-regions. These sub-regions can exchange heat, work, and mass with their surroundings through their own boundaries, and the entire process can be described by a set of differential equations. Based on the nodal analysis of the miniature pneumatic Stirling cryocooler and specific design parameters (as shown in Table 1), a one-dimensional model of the cryocooler is constructed using SAGE software.

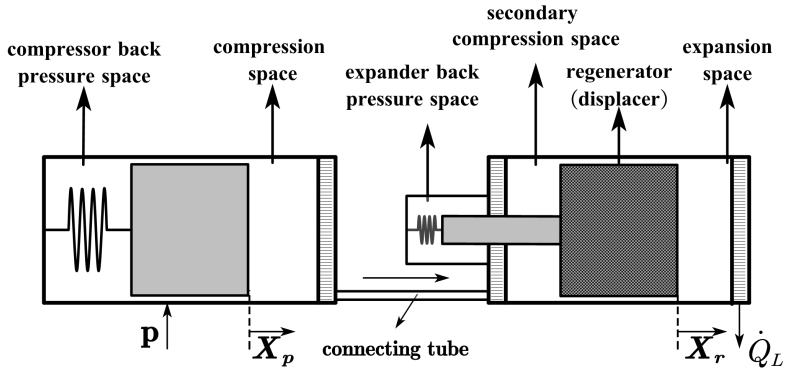


**Figure 1** Simplified Model of Miniature Pneumatic Stirling Cryocooler[38]

**Table 1** Partial Design Parameters of Miniature Pneumatic Stirling Cryocooler

| | Name | Parameter Values |
|---|---|---|
| Target Parameters | cooling capacity | ≥0.5 W |
| | refrigeration temperature | 77 K |
| Operating Parameters | pressure | 2.0 MPa |
| | frequency | 80-120 Hz |
| | input power | ≤25 W |
| Parts | compression space | Volume 0.302 $cm^3$ |
| | compressor back pressure space | Volume 1.563 $cm^3$ |
| | secondary compression space | Volume 0.068 $cm^3$ |
| | regenerator | Outer diameter 7.6 mm<br>Inner diameter 7.5 mm |

| | |
|---|---|
| | Length 38.6 mm |
| | 400# Stainless steel wire mesh |
| expansion space | Volume 0.091 $cm^3$ |
| expander back pressure space | Volume 0.628 $cm^3$ |

### 3.1 Internal Loss Distribution of Miniature Pneumatic Stirling Cryocooler

Figure 2 illustrates the distribution of internal energy losses in a split Stirling cryocooler. Among the four types of losses, the largest is due to flow resistance, accounting for 40% of the total losses, followed by non-ideal heat transfer losses at 35.6%, while conduction losses at 21.9% and shuttle losses at 2.5% are comparatively smaller. Concurrently, it is observed that the regenerator contributes the highest losses, constituting 50% of the total losses.
Secondly, irreversible losses generated in the connecting tubes can reach one-fifth of the total losses. Other components of the cryocooler produce irreversible losses below 10%, particularly within the working spaces, with the back pressure cavities of both components having negligible impact. In particular, the pumping loss, essentially an additional energy loss due to inadequate heat exchange between the gas and the walls within the clearance, can be attributed to the non-ideal heat transfer loss within the clearance and thus is not discussed separately.

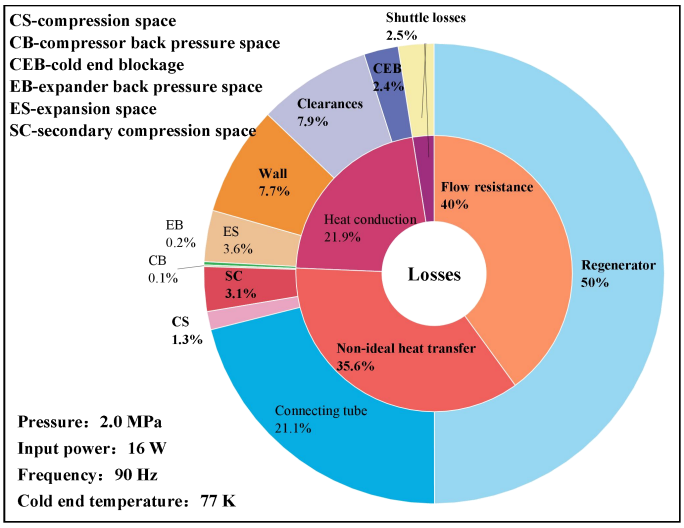


**Figure 2** Internal Loss Distribution Chart of Miniature Pneumatic Stirling Cryocooler

Figure 3 presents the variation curves of the three dominant losses, total losses, and cooling capacity with respect to frequency, demonstrating the significant influence of operating frequency on cooling performance and internal losses. As the frequency increases from 80 Hz to 110 Hz, the cooling capacity rises from 0.79 W to 087 W and then decreases to 0.62 W, peaking at 90 Hz. The trend of total flow resistance losses is opposite to that of the cooling capacity, achieving a minimum value at a frequency of 94 Hz. Meanwhile, the total axial conduction losses increase with frequency, but the trend for total non-ideal heat transfer losses is contrary.

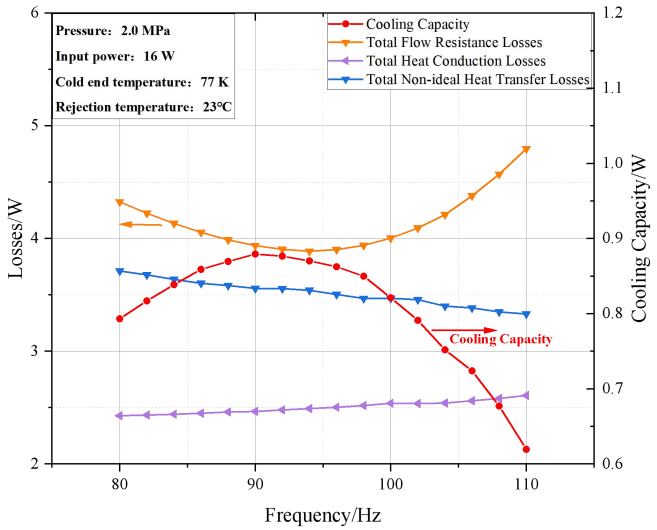


**Figure 3** The curve of total internal loss and cooling capacity of the refrigeration machine varying with frequency.

### 3.2 The Impact of Frequency on Internal Losses in the Regenerator

During the operation of the cryocooler, the internal conditions of the regenerator often deviate from the ideal state, leading to energy loss. The regenerator's heat exchange matrix, composed of a wire mesh, directly engages in heat exchange with the reciprocating working fluid. However, the thermal capacity of the metal mesh is not infinitely large as assumed in ideal conditions, which prevents the mesh from fully storing the heat from the gas or transferring all stored cold energy to the working fluid. This characteristic of non-ideal heat transfer results in entropy generation. Moreover, the wire mesh packed within the regenerator forms a non-uniform porous medium that partially impedes the flow of the working fluid. The viscous nature of the working fluid causes a reduction in pressure amplitude as it passes through the packing, leading to flow resistance losses. Additionally, axial conduction through the heat exchange matrix also contributes to certain conduction losses.

As depicted in Figure 4, while maintaining a constant filling pressure of 2.0 MPa, the pressure drop loss within the regenerator varies from 3.20 W to 2.39 W as the operating frequency is adjusted from 80 Hz to 110 Hz, reaching a minimum at 104 Hz. With the increase in operating frequency, the number of heat exchange occurrences between the working fluid and the heat exchange matrix per unit time correspondingly increases [39], leading to a reduction in non-ideal heat transfer loss from 1.95 W to 1.58 W. The maximum variation in axial conduction loss of the matrix is 20 mW. The total internal loss within the regenerator, which is the sum of the aforementioned three types of losses, gradually decreases with frequency and achieves a minimum at 108 Hz. The results indicate that moderately increasing the operating frequency can effectively reduce Non-ideal heat transfer losses, and there exists an optimal frequency that minimizes pressure drop losses. However, the axial loss of the heat exchange matrix does not exhibit significant variation with frequency changes.

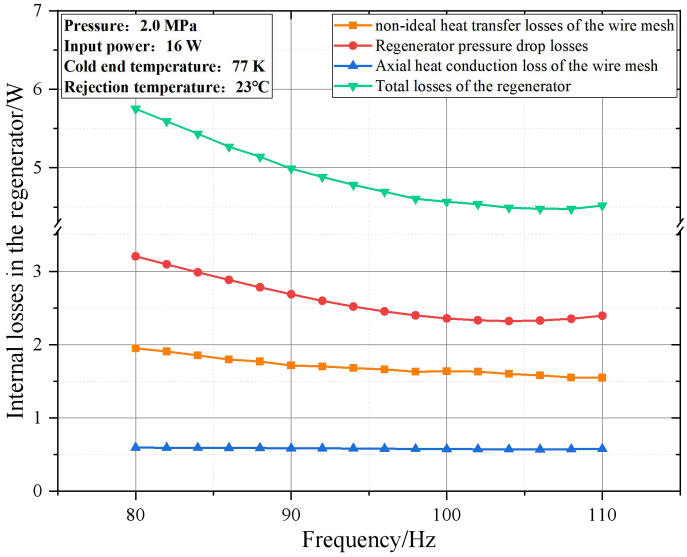


**Figure 4** The Curve of Internal Losses in the Regenerator Varying with Frequency

### 3.3 The Impact of Frequency on Internal Losses within the Connecting Tube

The interconnecting tube between the compressor and the expander is directly exposed to the external environment, allowing the working fluid passing through the thin walls to engage in heat exchange with the surroundings, leading to a substantial loss of energy through heat dissipation. Moreover, due to the small diameter and considerable length of the connecting tube, when the working fluid transitions from a larger volume space into the slender tube, the local and frictional resistances cause a reduction in pressure amplitude[40]. Figure 5 illustrates the variation curves of the pressure drop within the connecting tube, as well as the flow resistance and non-ideal heat transfer losses as a function of operating frequency. Notably, the pressure drop across the connecting tube increases rapidly with the rise in operating frequency, resulting in an increase in flow resistance loss from 0.85 W to 1.271 W, following a similar trend to the pressure drop. However, the increase in the number of heat exchange occurrences compensates for the non-ideal heat transfer; as the frequency rises from 80 Hz to 110 Hz, the heat exchange loss is reduced by 0.5 W. Nevertheless, since the pressure drop loss predominates within the connecting tube, the total loss exhibits an overall increasing trend with frequency.

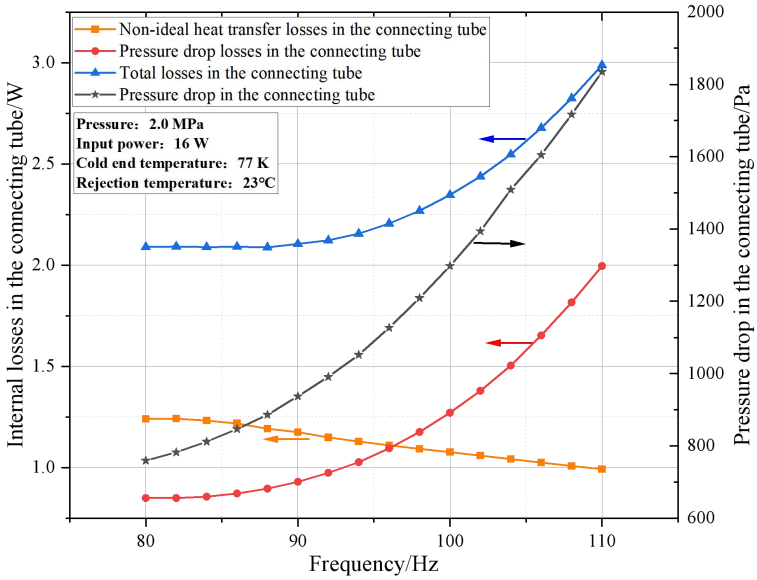


**Figure 5** The Curve of Internal Losses and Pressure Drop in the Connecting Tube Varying with Frequency

### 3.4 The Impact of Frequency on Losses in Clearances of Various Components

Clearance sealing, as one of the key technologies of linear Stirling cryocoolers, draws attention to the energy losses within the clearances. The most significant clearance losses are concentrated in the space between the regenerator and the cold finger wall. The fixed clearance volume between the displacer and the cylinder wall facilitates gas lubrication between the displacer and the cold finger wall; however, due to the viscous nature of the gas, frictional losses are inevitable. Additionally, since there are temperature gradients both axially and radially within the gap, heat exchange between the gap gas and the walls on either side, as well as with the cold end gas, is unavoidable. This alters the temperature of a portion of the heat in the regenerator and the expansion space gas to some extent, resulting in additional thermal loading.

Figure 6 illustrates the relationship between losses within various clearances and frequency variation. The total loss within the regenerator gap (the sum of shuttle loss and regenerator gap loss) significantly exceeds the clearance losses between the step shaft (displacer) and the compressor. As the frequency increases from 80 Hz to 110 Hz, losses in each gap tend to increase, indicating that a higher frequency leads to greater gap leakage. The shuttle loss fluctuates around 0.25 W and, since it depends on the operational characteristics of the regenerator and the temperature difference between the cold and hot ends, the displacer's travel will follow a similar pattern of change.

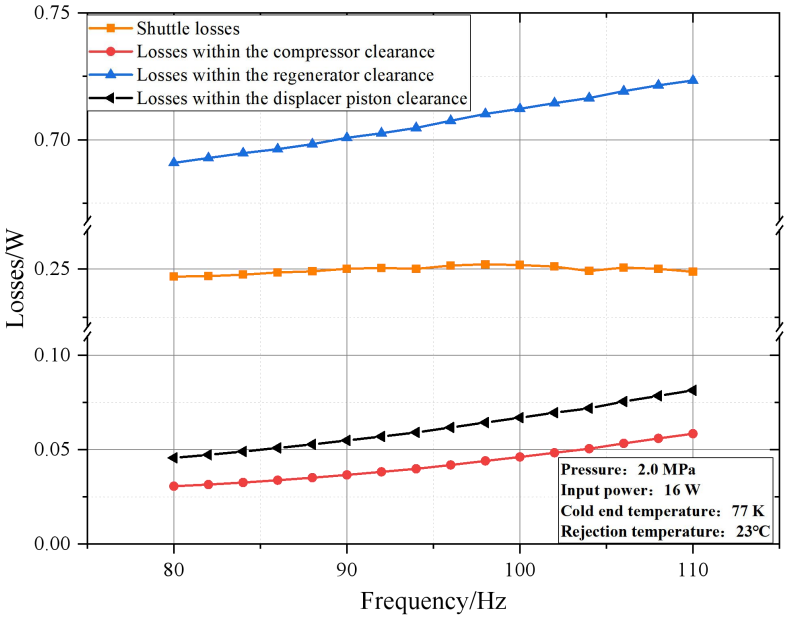


**Figure 6** The Curve of Internal Losses in the Clearances of Various Components Varying with Frequency

## 4 EXPERIMENTAL TESTING AND ANALYSIS

According to the simulation results, a miniature split Stirling cryocooler was designed and manufactured, followed by preliminary testing. It should be noted that the cryocooler was placed inside a temperature-controlled chamber, where the environmental temperature was regulated by adjusting the internal temperature of the chamber. The heat balance method was employed to test the cooling capacity. A heating element and temperature sensors were coupled inside the dewar, and once thermal equilibrium was achieved inside the dewar, the heating power value was numerically equal to the cooling capacity at the corresponding cold end temperature. Figure 7 presents the cooling curve under specific conditions, showing that under a certain heat load, the cold end temperature was reduced from 296 K to 77 K in 3.75 minutes, demonstrating the potential for rapid cooling of the Stirling cryocooler.

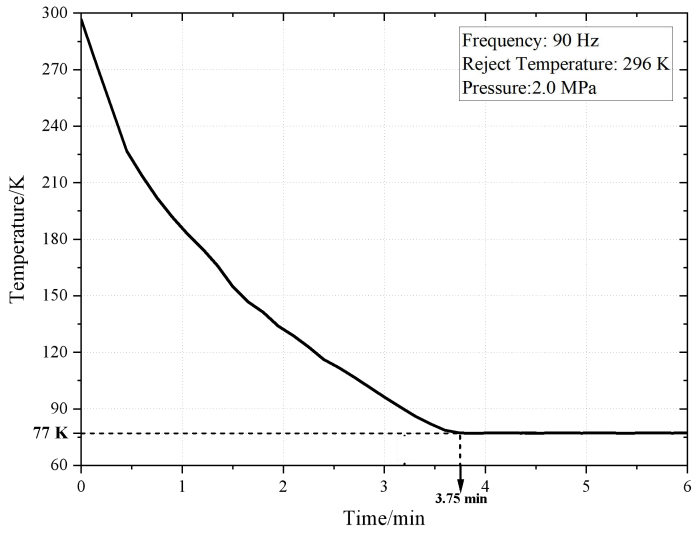


**Figure 7** The Cooling Curve of Miniature Stirling Cryocooler

Figure 8 illustrates the distribution of the cryocooler's cooling efficiency and compressor efficiency at different frequencies, as well as the cooling performance at the optimal frequency. Figure 8(a) further indicates that under an input power of 9 W, the COP distribution aligns with the simulated predicted trend, increasing with frequency and peaking at 90 Hz for optimal efficiency. The compressor efficiency varies with frequency in a similar manner to the cooling efficiency, but the frequencies corresponding to their peak efficiencies differ by 2 Hz. The compressor efficiency of around 80% suggests a suitable match between the compressor and the expander. Figure 8(b) presents the cryocooler's performance under high-temperature and room-temperature conditions. At a room temperature of 23℃, the cryocooler can achieve a cooling capacity of 905 mW@77 K@ 24.2 $W_{in}$. Notably, the cooling performance under high-temperature conditions is inferior to that under room temperature but still meets the demand for a cooling capacity of 500 mW. Under high temperatures, the regenerator cannot exchange heat with the surroundings as effectively as at lower temperatures, leading to a buildup of heat at the hot end and a reduction in cooling efficiency. Therefore, increasing heat exchange fins to enhance heat transfer is a simple yet effective extrinsic solution.

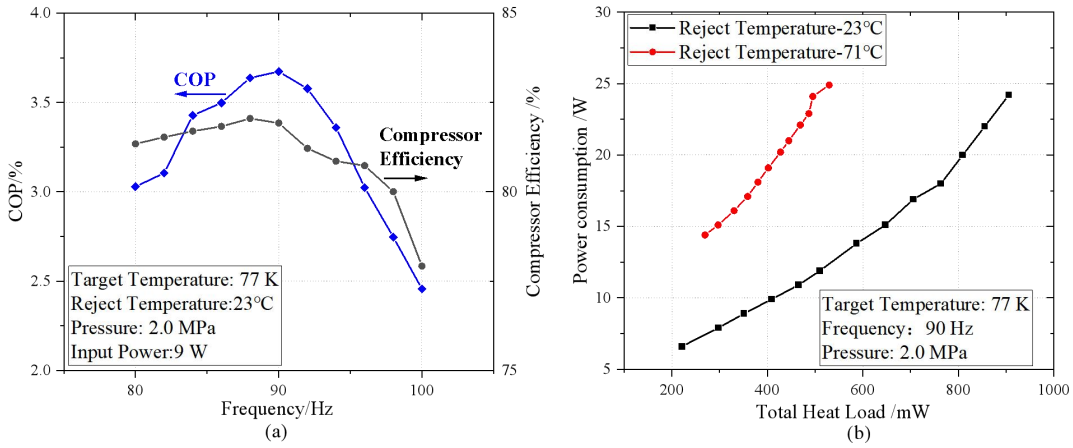


**Figure 8** The Actual Performance of the Miniature Stirling Cryocooler: (a) The Distribution of Cop and Compressor Efficiency with Frequency, (b) The Cooling Performance under High-Temperature and Room-Temperature Conditions

## 5 CONCLUSION

Through a detailed analysis of the internal losses in a 77K miniature pneumatic Stirling cryocooler, this study identifies

key factors affecting the cooling performance. Numerical simulation and experimental testing reveal that flow resistance loss is the most significant component of total losses, with non-ideal heat transfer loss and axial conduction loss also having a notable impact on cooling performance. The study further demonstrates that operating frequency significantly influences the distribution of internal energy losses and the cooling performance of the cryocooler. By adjusting the operating frequency, the resonant frequency of the cryocooler can be identified, thereby achieving optimal cooling performance. Experimental results validate the accuracy of the numerical model and show that the cryocooler achieves peak cooling performance at a frequency of 90 Hz. Additionally, the experiments indicate that the cooling performance of the cryocooler declines in high-temperature environments but can be improved by increasing heat exchange fins to enhance heat transfer efficiency. This research provides important theoretical guidance and experimental data support for the design, optimization, and application of miniature Stirling cryocoolers.

## COMPETING INTERESTS

The authors have no relevant financial or non-financial interests to disclose.

## REFERENCES

[1] Zhang Y, Wang X, Huang S, et al. Performance of a Highly Integrated Micro Linear Stirling Cooler with Active Vibration Cancellation. IOP Conference Series: Materials Science and Engineering, 2024: 130143. DOI: https://doi.org/10.1088/1757-899X/1301/1/012143.

[2] Xi Z, Zhang X, Jiang H. Heat-dynamics network model and energy analysis of a miniature free piston Stirling cryocooler for application of high operating temperature infrared detector. International Journal of Refrigeration, 2024. DOI: https://doi.org/10.1016/j.ijrefrig.2024.08.014.

[3] Han Y, Zhang A. Cryogenic technology for infrared detection in space. Scientific Reports, 2022, 12: 2349. DOI: https://doi.org/10.1038/s41598-022-06216-5.

[4] Willems D, Arts R, Buist J, et al. Synergies between designed-for-space and tactical cryocooler developments, ICC, 2018.

[5] Sun J, Zeng Y, Huang T, et al. A 150 K Micro Linear Split Stirling Cryocooler for High Operating Temperature Infrared Detectors. International Cryogenic Engineering Conference and International Cryogenic Materials Conference, Springer, 2022: 724–31. DOI: https://doi.org/10.1007/978-981-99-6128-3_94.

[6] Nussberger M, Zehner S, Withopf A, et al. Update on AIM HOT cooler developments. Infrared Technology and Applications XLV, 2019, 11002: 54-62. DOI: https://doi.org/10.1117/12.2520488.

[7] Yun L, Wei H, Wenfan Y, et al. HOT linear cooler developments at KIP. Third International Computing Imaging Conference (CITA 2023), 2023, 12921: 427–36. DOI: https://doi.org/10.1117/12.2688444.

[8] Arts R, Martin JY, Willems D, et al. Miniature cryocooler developments for high operating temperatures at Thales Cryogenics. SPIE Defense + Security, 2015. DOI: https://doi.org/10.1117/12.2176323.

[9] Arts R, Martin JY, Willems D, et al. Miniature Stirling cryocoolers at Thales Cryogenics: qualification results and integration solutions. SPIE Defense + Security, 2016. DOI: https://doi.org/10.1117/12.2228681.

[10] Willems D, Veer BD, Arts R, et al. High-availability single-stage Stirling coolers with high power density. IOP Conference Series Materials Science and Engineering, 2020, 755: 012044. DOI: https://doi.org/10.1088/1757-899X/755/1/012044.

[11] Filis A, Carmiel M, Nachman I. Ricor's advanced rotary and linear miniature cryocoolers for HOT IR detectors. Defense + Commercial Sensing, 2022.

[12] Veprik A, Vilenchik H, Riabzev S, et al. Microminiature linear split Stirling cryogenic cooler for portable infrared imagers. Infrared Technology and Applications XXXIII, 2007, 6542: 823–34. DOI: https://doi.org/10.1117/12.715622.

[13] Veprik A, Gedeon D, Radebaugh R, et al. Low-cost cryogenic technologies for high-operating temperature infrared imaging. Infrared Technology and Applications XLIX, 2023, 12534: 60–77. DOI: https://doi.org/10.1117/12.2664389.

[14] Veprik A, Refaeli R, Wise A, et al. Disruptive cryocoolers for commercial IR imaging. Infrared Technology and Applications XLVIII, 2022, 12107: 120–32. DOI: https://doi.org/10.1117/12.2618257.

[15] Mabrouk MT, Kheiri A, Feidt M. Effect of leakage losses on the performance of a β type Stirling engine. Energy, 2015, 88:111–7. DOI: https://doi.org/10.1016/j.energy.2015.05.075.

[16] Li R, Grosu L, Queiros-Conde D. Multi-objective optimization of Stirling engine using Finite Physical Dimensions Thermodynamics (FPDT) method. Energy Conversion and Management, 2016, 124: 517–27. DOI: https://doi.org/10.1016/j.enconman.2016.07.047.

[17] Hachem H, Gheith R, Aloui F, et al. Technological challenges and optimization efforts of the Stirling machine: A review. Energy Conversion and Management, 2018, 171: 1365–87. DOI: https://doi.org/10.1016/j.enconman.2018.06.042.

[18] Parlak N, Wagner A, Elsner M, et al. Thermodynamic analysis of a gamma type Stirling engine in non-ideal adiabatic conditions. Renewable Energy, 2009, 34: 266–73. DOI: https://doi.org/10.1016/j.renene.2008.02.030.

[19] Swift GW. Thermoacoustics: A unifying perspective for some engines and refrigerators. Springer, 2017.

[20] Wang B, Guo Y, Chao Y, et al. Acoustic-Mechanical-Electrical (AcME) coupling between the linear compressor and the Stirling-type cryocoolers. International Journal of Refrigeration, 2019, 100: 175–83. DOI: https://doi.org/10.1016/j.ijrefrig.2019.01.023.
[21] Bo W, Yijun C, Haoren W, et al. A miniature Stirling cryocooler operating above 100 Hz down to liquid nitrogen temperature. Applied Thermal Engineering, 2021, 186: 116524. DOI: https://doi.org/10.1016/j.applthermaleng.2020.116524.
[22] Getie MZ, Lanzetta F, Bégot S, et al. Reversed regenerative Stirling cycle machine for refrigeration application: A review. International Journal of Refrigeration, 2020, 118: 173–87. DOI: https://doi.org/10.1016/j.ijrefrig.2020.06.007.
[23] Ahmadi MH, Ahmadi M-A, Pourfayaz F. Thermal models for analysis of performance of Stirling engine: A review. Renewable and Sustainable Energy Reviews, 2017, 68: 168–84. DOI: https://doi.org/10.1016/j.rser.2016.09.033.
[24] Hachem H, Gheith R, Aloui F, et al. Optimization of an air-filled Beta type Stirling refrigerator. International Journal of Refrigeration, 2017, 76: 296–312. DOI: https://doi.org/10.1016/j.ijrefrig.2017.02.019.
[25] Li R, Grosu L. Parameter effect analysis for a Stirling cryocooler. International Journal of Refrigeration, 2017, 80:92–105. DOI: https://doi.org/10.1016/j.ijrefrig.2017.05.006.
[26] Tanaka M, Yamashita I, Chisaka F. Flow and heat transfer characteristics of the Stirling engine regenerator in an oscillating flow. JSME International Journal Ser 2, Fluids Engineering, Heat Transfer, Power, Combustion, Thermophysical Properties, 1990, 33: 283–9. DOI: https://doi.org/10.1299/jsmeb1988.33.2_283.
[27] Rohsenow WM, Hartnett JP, Ganic EN. Handbook of heat transfer fundamentals, 1985.
[28] Gedeon D, Wood JG. Oscillating-flow regenerator test rig: hardware and theory with derived correlations for screens and felts. 1996.
[29] Li R, Grosu L, Queiros-Conde D. Multi-objective optimization of Stirling engine using Finite Physical Dimensions Thermodynamics (FPDT) method. Energy Conversion and Management, 2016, 124: 517–27. https://doi.org/10.1016/j.enconman.2016.07.047.
[30] Pfeiffer J, Kuehl H-D. Optimization of the appendix gap Design in Stirling Engines. Journal of Thermophysics and Heat Transfer, 2016, 30: 831–42. DOI: https://doi.org/10.2514/1.T4729.
[31] Segado MA, Brisson JG. Appendix Gap Losses with Pressure-Driven Mass Flows. ICC, 2012.
[32] Strauss JM, Dobson RT. Evaluation of a second order simulation for Sterling engine design and optimisation. Journal of Energy in Southern Africa, 2010, 21: 17–29.
[33] Shendage D, Kedare S, Bapat S. Cyclic analysis and optimization of design parameters for Beta-configuration Stirling engine using rhombic drive. Applied Thermal Engineering, 2017, 124: 595–615. DOI: https://doi.org/10.1016/j.applthermaleng.2017.06.075.
[34] Mahmoodi M, Pirkandi J, Alipour A. Numerical simulation of beta type stirling engine considering heat and power losses. Iranian Journal of Mechanical Engineering Transactions of the ISME, 2014, 15: 5–27. DOI: https://doi.org/20.1001.1.16059727.2014.15.2.1.4.
[35] Cun-Quan Z, Yi-Nong W, Guo-Lin J, et al. Dynamic simulation of one-stage Oxford split-Stirling cryocooler and comparison with experiment. Cryogenics, 2002, 42: 577–85. DOI: https://doi.org/10.1016/S0011-2275(02)00098-X.
[36] Timoumi Y, Tlili I, Nasrallah SB. Design and performance optimization of GPU-3 Stirling engines. Energy, 2008, 33: 1100–14. DOI: https://doi.org/10.1016/j.energy.2008.02.005.
[37] Getie MZ. Numerical modeling and optimization of a regenerative Stirling refrigerating machine for moderate cooling applications. PhD Thesis. Université Bourgogne Franche-Comté, 2021.
[38] Waele ATAM de, Liang W. Basic dynamics of split Stirling refrigerators. Cryogenics, 2008, 48: 417–25. DOI: https://doi.org/10.1016/j.cryogenics.2008.04.004.
[39] Srinivasan KV, Manimaran A, Arulprakasajothi M, et al. Design and development of porous regenerator for Stirling cryocooler using additive manufacturing. Thermal Science and Engineering Progress, 2019, 11: 195–203. https://doi.org/10.1016/j.tsep.2019.03.013.
[40] Liu S, Jiang Z, Ding L, et al. Impact of operating parameters on 80 K pulse tube cryocoolers for space applications. International Journal of Refrigeration, 2019, 99: 226–33. DOI: https://doi.org/10.1016/j.ijrefrig.2018.12.026.